

# **DERIVATION OF GLOBAL GCM BOUNDARY CONDITIONS FROM 1 KM LAND USE SATELLITE DATA**

**STEFAN HAGEMANN<sup>\*</sup>, MICHAEL BOTZET, LYDIA DÜMENIL AND  
BENNERT MACHENHAUER**

Max Planck Institute for Meteorology  
Bundesstraße 55  
D-20146 Hamburg, Germany

<sup>\*</sup>e-mail: [Hagemann@dkrz.de](mailto:Hagemann@dkrz.de)  
<http://www.mpimet.mpg.de/privat/Mitarbeiter/hagemann.stefan>  
Tel.: +49-40-41173-101  
Fax: +49-40-41173-366

**MPI Report No. 289**

March 1999

**ISSN 0937-1060**

# Contents

|                                                        |           |
|--------------------------------------------------------|-----------|
| <b>Abstract</b> .....                                  | <b>3</b>  |
| <b>1. Introduction</b> .....                           | <b>4</b>  |
| <b>2. Allocation of land surface parameters</b> .....  | <b>6</b>  |
| 2.1. Surface albedo .....                              | 6         |
| 2.2. Roughness length due to vegetation .....          | 7         |
| 2.3. Fractional vegetation and leaf area index .....   | 8         |
| 2.4. Forest ratio .....                                | 9         |
| 2.5. Soil water holding capacity .....                 | 10        |
| <b>3. Aggregation of land surface parameters</b> ..... | <b>12</b> |
| 3.1. Aggregation of roughness length .....             | 12        |
| <b>4. Discussion of the new datasets</b> .....         | <b>14</b> |
| 4.1. Global view .....                                 | 14        |
| 4.2. Regional view at Europe .....                     | 16        |
| <b>5. Conclusions</b> .....                            | <b>18</b> |
| Acknowledgements .....                                 | 18        |
| <b>References</b> .....                                | <b>19</b> |

## **Abstract**

The coupling between atmosphere and biosphere is of particular importance over land surfaces from both the atmospheric and hydrological point of view. For an adequate modelling of processes at the land surface boundary to the atmosphere an accurate representation of the land surface is necessary. The description of the present land surface is a significant problem in global and regional climate modelling. The available datasets are particularly inaccurate in some regions of the world and up to now their spatial resolution was too coarse to fit the demands of high resolution limited area models. Recent development in remote sensing facilitates the measurement of present land surface characteristics at a very fine spatial resolution thereby offering the possibility to create new datasets of land surface parameters for numerical modelling.

At a resolution of 1 km a global distribution of major ecosystem types (according to *Olson*, 1994a, 1994b) was recently made available by the U.S. Geological Survey. It was derived from International Geosphere Biosphere Programme 1 km AVHRR data. From this global distribution a global dataset of land surface parameters is constructed by allocating parameters to each ecosystem type. These parameters are: background surface albedo, surface roughness length due to vegetation, fractional vegetation cover and leaf area index for the growing and dormancy season, forest ratio, plant-available soil water holding capacity, and volumetric wilting point. This global dataset is provided for the use in global and regional climate modelling.

## 1. Introduction

The coupling between atmosphere and biosphere is of particular importance over land surfaces from both the atmospheric and hydrological point of view. For an adequate modelling of processes at the land surface boundary to the atmosphere an accurate representation of the land surface is necessary. A model used to simulate these processes requires a proper determination of the land surface characteristics that are used in its parameterizations as boundary conditions. Therefore, the description of the land surface is a significant problem in global and regional climate modelling since deficiencies or inconsistencies in these boundary conditions may lead to errors in the climate simulations.

As stated in a review by *Rowntree* (1991), numerous numerical climate simulations have shown that anomalies in albedo and surface roughness can produce significant changes in the atmospheric circulation. *Pielke et al.* (1997) have demonstrated that the landscape, including its spatial heterogeneity, has a substantial influence on the overlying atmosphere. An adequate determination of land surface characteristics dependent on plant canopies is of particular importance because they strongly modify the evapotranspiration over large areas of the land surface which is a major component of the surface thermal and moisture balance and of the hydrological cycle.

Thus the assessment of new or improved land surface datasets was central to a number of programs and experiments, e. g. the ‘International Satellite Land-Surface Climatology Program’ (ISLSCP) and the ‘International Geosphere-Biosphere Program’ (IGBP). For an overview about these programs and experiments, see *Feddes et al.* (1998).

One of the first archives of global land surface datasets was prepared by *Henderson-Sellers et al.* (1986) at resolutions ranging from 1x1 to 5x5 degree. This archive comprises of a collection of several data sources (e.g. *Matthews*, 1983; *Olson et al.*, 1983; *Wilson*, 1984; soil data of *Gildea and Moore*, 1985, based on *FAO/Unesco*, 1971-1981; *Cogley*, 1986). Most of these data sources are based on maps and literature. A very large database was collected during the ‘ISLSCP Initiative I’ (*Meeson et al.*, 1995). In this database, most of the published global datasets of land surface characteristics have a spatial resolution of 1 degree.

The spatial resolution of the currently available datasets is too coarse to fit the demands of high resolution limited area models, since the resolution used in regional climate simulations usually ranges from 0.1 degree to 0.5 degree. Also, these datasets are most probably inaccurate in some parts of the world. *Henderson-Sellers et al.* (1986) stated that their collected datasets are inconsistent to each other in several regions. For instance, the ecosystem data of *Olson et al.* (1983) localize vegetation at the coastal regions of Morocco and Tunisia that reach far into the land which is unrealistic (e.g. as compared to *Diercke*, 1988, 1992). *Hagemann and Dümenil* (1999) found out that the wetlands distributions of *Matthews and Fung* (1987) and *Cogley* (1987, 1991, 1994; taken from ISLSCP) differ largely.

Recent development in remote sensing facilitates the measurement of present land surface characteristics at a very fine spatial resolution thereby offering the possibility to create consistent land surface boundary conditions for numerical models. In IGBP, 10-day composites of spectral radiances from an Advanced Very High Resolution Radiometer (AVHRR) have been made available from April 1992 to March 1993 at 1 km resolution

(Eidenshink and Faundeen, 1994). These data were used by the *U.S. Geological Survey* (1997) to derive a global distribution of major ecosystem types according to the definitions given by *Olson* (1994a, 1994b).

This technical note describes the construction of a global dataset of land surface parameters based on this 1 km ecosystem type distribution. The set of the chosen parameters (background surface albedo, surface roughness length due to vegetation, fractional vegetation cover and leaf area index for the growing and dormancy season, forest ratio, plant-available soil water holding capacity, and volumetric wilting point) was defined by the parameters that are used or shall be used in the climate models of the Max Planck Institute for Meteorology (MPI). The dataset is constructed by allocating a specific set of parameters to each ecosystem type. The allocation methods for the different parameters are described in Sect. 2.

The 1 km data will be aggregated to a grid resolution ranging from 0.1 degree for limited area models to T106 (ca. 1.1°) or T42 (ca. 2.8°) for atmospheric general circulation models (GCMs) at MPI. The same technique of aggregation can not be used for all land surface parameters. Thus, Sect. 3 deals with the issue of aggregation.

In Sect. 4, the new land surface parameters are compared to the old ones used at MPI and checked for plausibility.

## 2. Allocation of land surface parameters

*Olson et al.* (1983) constructed a global distribution of major ecosystem complexes that has a resolution of 0.5 degree. The dataset contains 45 different ecosystem types. By allocating specific parameter values to each of the ecosystem complexes, *Claussen et al.* (1994) derived a global dataset of biosphere related land surface parameters. They generated 0.5 degree fields in a regular grid for background (surface) albedo, surface roughness length due to vegetation, leaf area index, fractional vegetation cover, and forest ratio. These fields are currently used in the MPI climate models, the GCM ECHAM4 (*Roeckner et al.*, 1996) and the regional climate models HIRHAM4 (*Christensen et al.*, 1996) and REMO with ECHAM4 physics (*Jacob and Podzun*, 1997). In this study, we use the same allocation method as *Claussen et al.* (1994).

As mentioned in Sect. 1, the U.S. Geological Survey has constructed their global 1 km distribution of major ecosystem types according to a classification list of *Olson* (1994a, 1994b). Compared to the old classification list presented in *Olson et al.* (1983), *Olson* (1994a, 1994b) has increased the number of ecosystem types (from 45 to 94) but only 70 of the new 94 ecosystem types are included in the 1 km dataset.

In the present work, the allocation of land surface parameters to the new ecosystem types is conducted to facilitate the generation of a global dataset of these parameters at 1 km and coarser resolutions. For ecosystem types that are included in both classification lists, initially the same parameter values as in *Claussen et al.* (1994) were allocated. For each of the other ecosystem types, parameter values were assigned that correspond to a similar type of the old list. According to this method, parameter allocations are done for background (surface) albedo (see Sect. 2.1), surface roughness length due to vegetation (see Sect. 2.2), fractional vegetation cover and leaf area index (see Sect. 2.3), and forest ratio (see Sect. 2.4). The corresponding parameter values are shown in Table 1.

Since *Claussen et al.* (1994) characterized their allocations for leaf area index, fractional vegetation cover and forest ratio as very rough estimates, a method is developed that improves these rough estimates (see Sect. 2.3). For some regions of the earth, corrections have to be applied for particular ecosystems types.

Beyond the parameters that are already treated, soil water holding capacities are assigned to each ecosystem type to achieve a consistent global capacity dataset. Sect. 2.5 deals with this issue. The corrected and improved parameter values are shown in Table 2.

### 2.1. Surface albedo

The background (surface) albedo  $a_s$  is a measure of the ability of the model land surface to reflect the incoming solar radiation on snowfree areas. Therefore it is an important parameter in the model equations that describe radiation processes at the atmosphere-land surface boundary.

In this study, the allocations of  $a_s$  to ecosystem types are based solely on *Claussen et al.* (1994). Their 0.5 degree albedo dataset was merged with observed data of the ‘Earth Radiation Budget Experiment’ (ERBE; *Ramanathan et al.*, 1989) which have a very coarse spatial resolution of 2.5°. In the new data, each parameter distribution is based only on the allocation of parameter values to land use types. This offers the possibility to easily derive different parameter distributions by changing the land use types distribution as it may be desired in experiments using different (e. g. future or paleo-climatic) boundary conditions. Thus, a merging of the new  $a_s$  values with the ERBE data is not adopted. This may lead to some deviations from actual albedo values in regions that are mainly covered with bare soil. In particular in the bare desert regions of the Sahara and Saudi Arabia the albedo obtained is too low compared to observed data of ERBE (*Barkstrom et al.*, 1990) and calculated data of *Sellers et al.* (1995a, 1995b) that are based on Normalized Difference Vegetation Index (NDVI) data and GCM computations. Therefore a value of 0.35, which seems to be a representative value according to these two datasets, is assigned to bare desert in these regions.

## 2.2. Roughness length due to vegetation

The roughness length  $z_0$  is a measure of the roughness of the surface used to describe processes in the surface boundary layer (in the Prandtl layer, the wind velocity becomes independent of the Reynolds number and the wind speed depends logarithmically on the height above the surface; *Mason*, 1987). In the models, the turbulent exchange of momentum, energy, and moisture between the surface and the atmosphere is calculated as a function of  $z_0$ . In areas of low orography, the vegetation part of the roughness length often controls this mixing (*Henderson-Sellers et al.*, 1986). Thus, the roughness length  $z_0$  consists of two parts: a roughness length  $z_{0,oro}$  computed from the variance of orography, and a roughness length  $z_{0,veg}$  of vegetation and land use. According to *Tibaldi and Geleyn* (1981), the square of  $z_0$  equals the sum of the squares of  $z_{0,oro}$  and  $z_{0,veg}$ .

For the roughness length  $z_{0,veg}$ , no corrections were made to the new allocations. Urban areas are not covered by the ecosystem types considered in *Claussen et al.* (1994). Thus, a value of 2.5 m is assigned as proposed by *Tibaldi and Geleyn* (1981). In contrast to these authors, we consider urban areas as one of the land use types used in the computation of  $z_{0,veg}$  instead of treating it as a separate term (as done with  $z_{0,oro}$ ) in the computation of  $z_0$  (see above). The roughness length over the oceans is computed in the climate model depending on wind speed. But this is usually not done for land gridboxes in the climate model that are partially covered with water. Here, following *Claussen* (1991), we set a roughness value<sup>1</sup> of 0.0002 m.

---

1. In ECHAM4 (*Roeckner et al.*, 1996), the minimum value of  $z_{0,veg}$  over water is set to  $1.5 \cdot 10^{-5}$  m, and the BATS model (*Dickinson et al.*, 1993) uses a value of  $2.3 \cdot 10^{-4}$ .

### 2.3. Fractional vegetation and leaf area index

Small variable openings in the leaves of plants, known as stomata, control the flow of water vapour between the leaf and the outside air. Such a control is commonly referred to as stomatal resistance in analogy with Ohm's law for the electric resistance. A certain vegetation canopy may consist of several canopy layers. Therefore the canopy usually has a surface area greater than its projected area on the ground. The ratio of the leaf area to the projection is known as the leaf area index (LAI) and can be used to relate the stomatal resistance to a resistance of the canopy. The fractional vegetation  $c_v$  indicates the fractional area covered by plants within a gridbox which are able to modify evapotranspiration by their stomata.

Apart from its influence on the evapotranspiration via the surface resistance of the canopy, the LAI defines also the size of the precipitation interception capacity (skin reservoir). Although interception capacities are small compared to soil water holding capacities, their effect can be quite large as intercepted rainfall can evaporate at the potential rate. The effect is greatest when there are frequent low intensity rainfall events. The soil remains drier than it would without a canopy store, and evaporation is larger (Warrilow *et al.*, 1986).

For  $c_v$  and LAI, we have allocated maximum and minimum values valid for the growing and dormancy season, respectively, to each land use type. Claussen *et al.* (1994) stated that their allocations of  $c_v$  and LAI are provisional and that it seems more reasonable to infer  $c_v$  and LAI from data of net primary production of vegetation.

Since appropriate global data of  $c_v$  and LAI are not available, a different data source had to be found to improve  $c_v$  and LAI. According to the Beer-Lambert's law (Monsi and Saeki, 1953), the fraction of photosynthetic absorbed radiation  $f_{PAR}$  is closely connected to  $c_v$  and LAI by Eq. (1).

$$f_{PAR} = c_v \cdot \left( 1 - e^{-\left(0.5 \cdot \frac{LAI}{c_v}\right)} \right) \quad (1)$$

Knorr (1997, 1998) has derived a global distribution of  $f_{PAR}$  from data of Berthelot *et al.* (1994) based on NOAA/AVHRR data at 0.5 degree resolution.

In order to allocate  $f_{PAR}$  values to ecosystem types (taken from the 1 km dataset), all gridboxes were considered where the fractional coverage of a specific ecosystem type is larger than a certain threshold value at 0.5 degree resolution. It is assumed that for such gridboxes the corresponding  $f_{PAR}$  value is typical for the specific ecosystem type. Four different threshold values (60%, 70%, 80% and 90%) were used to account for different maximum spatial coverages of the ecosystem types. For each ecosystem type for which such gridboxes exist, the  $f_{PAR}$  values located in the corresponding gridboxes of the 0.5 degree  $f_{PAR}$  distribution were averaged and assigned to the ecosystem type for each of the four threshold values. This was done separately for the maximum values of  $f_{PAR}$  (that correspond to the growing season) and for the minimum values of  $f_{PAR}$  (that correspond to the dormancy season). The latter values are more scarce since during winter time large parts of the northern hemisphere are covered by

snow that does not allow an accurate measurement of  $f_{PAR}$ . By examining the averaged  $f_{PAR}$  values, specific values of  $f_{PAR}$  were assigned to most of the ecosystem types for both seasons. If the assignment of a  $f_{PAR}$  value was not possible for a specific ecosystem type and a particular season the initial values were kept for  $c_v$  and LAI.

Eq. (1) is not sufficient to derive both  $c_v$  and LAI from the correlated values of  $f_{PAR}$ . Thus as a second criterion, the relative change from the initial values to the corrected values of  $c_v$  and LAI are forced to be minimized. This means that the changes must satisfy Eq. (2):

$$\left(\frac{\Delta c_v}{c_v}\right)^2 + \left(\frac{\Delta LAI}{LAI}\right)^2 = \text{Minimum} \quad (2)$$

For some regions, however, the initial unchanged values of  $c_v$  and LAI of a particular ecosystem type are used as suggested by Knorr (personal communication, 1998). This is done for *Cold Grassland* in the Andes for the growing season, *Cool Crops & Towns* in Canada and middle west of the USA for the dormancy season, *Succulent and Thorn Shrub* in north-east Brazil for both seasons, *Crops, Grass, Shrubs* in South America for the growing season.

For *Low Sparse Grassland* and *Cold Grasses and Shrubs* in the southern part of South America,  $c_v$  of the growing season is set to 0.15 since this region is very sparsely vegetated. The corresponding LAI is set to the initial value. For *Tropical Rainforest*, the correction yields the same values as the initial ones except for  $c_v$  in the dormancy season. Knorr (1997) stated that there are some data problems over the South American rainforest due to large water vapour contents of the atmosphere, so therefore the initial value is kept. For *Crops and Towns* and *Forest and Fields* in central and southern Spain,  $c_v$  and LAI of the growing season were modified based solely on considerations of  $f_{PAR}$  in this region. For the first we set  $c_v = 0.6$  and LAI = 2.5, for the latter we set  $c_v = 0.65$  and LAI = 4.

It is important to note that in the dormancy season the distribution of  $f_{PAR}$  possesses a very large amount of missing data. Thus, the corrections made for the dormancy season may have a lesser accuracy than the corrections for the growing season.

## 2.4. Forest ratio

The forest ratio  $c_f$  is the fractional cover of trees, regardless whether they are photosynthetically active or not. Thus, in winter  $c_v$  may become smaller than  $c_f$  for deciduous plants. In the summer and for evergreen plants throughout the year,  $c_f \leq c_v$  should be valid. In the MPI climate model,  $c_f$  is used to account for the different behaviour of the snow albedo in forested and non-forested areas. Also,  $c_f$  has the potential of being used for other snow dependent characteristics such as snowmelt (e.g. done in the HBV model of *Bergström*, 1992).

*Claussen et al.* (1994) have specified the forest ratio  $c_f$  consistent with fractional vegetation  $c_v$ . Therefore the initial allocation is done in the same way as for the allocation of the  $c_v$  values (see Sect. 2.3). For land use types where  $c_v$  is corrected, the corresponding forest ratio is corrected in an analogous way by applying the same correction factor. For *Woody Savannah*, the initial value is used since the correction would yield an unrealistic high value of  $c_f$ . As for  $c_v$  and LAI (cf. Sect. 2.3), the initial value of  $c_f$  is also used for *Succulent and Thorn Shrub* in north-eastern Brazil.

## 2.5. Soil water holding capacity

Different terms exist to describe the maximum amounts of water that may be stored in the soil. The total amount of water that may be stored due to the porosity of the soil is the pore volume. This volume may be totally filled only for a very short time after a heavy rain event (except for wetlands, see also Sect. 4.1). The field capacity  $W_{cap}$  is the amount of water held in an originally saturated soil by capillary forces after several days of drainage. The plant available water capacity  $W_{ava}$  is the maximum amount of water that plants may extract from the soil before they start to wilt. The difference of  $W_{cap}$  and  $W_{ava}$  is called the permanent wilting point  $W_{pwp}$ .  $W_{ava}$  is climatologically important because it defines the maximum soil moisture that is potentially available to the atmosphere due to the transpiration of plants.  $W_{cap}$  is also quite important inasmuch as it is necessary in establishing the mass conservation of the hydrological cycle, thereby determining the turnover of precipitation into evaporation, and in controlling runoff and drainage processes.

The soil water holding capacity is one of the most uncertain parameters in global and regional climate modelling. The definition of the water holding capacity used in a climate model is model dependent and has to be consistent with the model's formulation of evaporation processes (*Schulz et al.*, 1998). The exact definition of this capacity may be crucial for the simulation of the hydrological cycle and its influence in the model simulations. Also the determination of the soil water holding capacity for a given area is a difficult task, since it cannot be measured on a larger area so far. First, the relative capacity has to be determined, which is defined as capacity volume per depth, and second, the depth over which the relative capacity has to be integrated to yield the total soil water holding capacity must be determined. Since the soil is usually very heterogeneous, a value given for a certain place can only be an estimate of the capacity that is representative for the area. Therefore one could not expect to find a perfect algorithm that allows an exact determination of the soil water holding capacities everywhere on the globe.

The current version of ECHAM4 (*Roeckner et al.*, 1996) uses field capacities  $W_{cap}$  as maximum soil water holding capacities according to a  $0.5^\circ$  dataset of *Patterson* (1990). *Kleidon* (1998a, b) stated that these capacities are too low for many regions of the Earth, especially in the tropics. *Hagemann and Kleidon* (1998) have compared three different climate simulations of the GCM ECHAM4 at T42 resolution: a control experiment, a simulation using field capacities based on the assumption of shallow roots in the tropics, and a simulation using field capacities based on optimized (deep) rooting depths in the tropics which are generally

deeper than those of the control experiment. Their study reveals that the simulation with the deepest rooting depths (corresponding to the largest field capacities) is in general closest to observations. In their paper, they also discuss the effects of different rooting depths and thus field capacity on the simulated hydrologic cycle of the GCM.

$$f_{pwp} = \frac{W_{cap} - W_{ava}}{W_{cap}} \quad (3)$$

ECHAM4 uses a constant value of the volumetric wilting point  $f_{pwp}$  (defined by Eq. (3)) of 35%. It may be useful to replace this constant value by a global spatially varying dataset of  $f_{pwp}$ . Such a dataset may be easily derived from 0.5° datasets of  $W_{cap}$  and  $W_{ava}$  according to *Patterson* (1990).

In order to achieve a high resolution dataset of soil water holding capacities that is consistent with the other vegetation-related parameter fields, we have assigned values of  $W_{ava}$  and  $f_{pwp}$  to each land cover type. For some regions this may be not very realistic since the soil water capacities depend on the texture of the soil which is not as highly correlated with a land cover type as a pure vegetation parameter. *Dunne and Wilmott* (1996) stated that the most influential and uncertain parameter for the determination of soil water capacities is the depth over which  $W_{ava}$  is computed. This depth is usually limited by root depth. Soil texture exerts a lesser, but still substantial, influence. Organic content, except where concentrations are very high, has relatively little effect. Since the parameter primarily influencing  $W_{ava}$  is root depth which depends largely on the land use type, the assignment of  $W_{ava}$  to land cover types seems to be reasonable. Also the achieved consistency may compensate a weakness of this kind of allocation to a certain degree.

The allocation of  $f_{pwp}$  and  $W_{ava}$  to the land cover types should be based on correlations of the land cover types with 0.5 degree datasets of  $f_{pwp}$  and  $W_{ava}$  that are done in the same way as for  $f_{PAR}$  in Sect. 2.3. But the choice of appropriate soil water capacity data was not an easy task. As mentioned above, the capacity fields of  $W_{cap}$  and  $W_{ava}$  of *Patterson* (1990) are generally too small. But it seems that the derived distribution of  $f_{pwp}$  from these capacity fields is quite realistic, so that these  $f_{pwp}$  data were chosen.

Second, a global 0.5 degree dataset of  $W_{ava}$  was chosen which was constructed by *Kleidon* (personal communication, 1998) based on optimized rooting depths (*Kleidon and Heimann*, 1998c). In this approach, the benefit of the vegetation - expressed by the net primary productivity as simulated by a terrestrial biosphere model - is maximized in respect to rooting depth expressing optimum adaptation of the vegetation to its climatic environment. The calculated global distribution of rooting depth compares well with the general pattern for vegetation types obtained from observations of maximum rooting depths (*Canadell et al.*, 1996). To correct for deficiencies (especially with respect to the *Tundra* vegetation type), optimized rooting depths are constrained by the minimum and maximum values of rooting depth reported for all species within one vegetation type (*Canadell et al.*, 1996) using the vegetation classification of *Wilson and Henderson-Sellers* (1985) and the soil texture information of *Batjes* (1996) that is based on FAO soil data.

### 3. Aggregation of land surface parameters

The majority of global climate models (GCMs) assume land surfaces to be homogeneous within GCM grid cells, typically ranging from 100x100 to 500x500 km<sup>2</sup>. Thus, the subgrid-scale heterogeneity of land surfaces, on a wide spectrum of length scales, poses a main problem in global climate modelling. This problem can be tackled by considering a large, heterogeneous area, such as a GCM grid cell, to be made up of a number of different land surface types which together constitute a ‘mosaic’ of ‘tiles’ (such as done in the SECHIBA land surface scheme; *Ducoudre et al.*, 1993). Four general approaches exist, as suggested by *Feddes et al.* (1998):

- to define the surface characteristics of the tiles, either from high resolution data (e.g. from remote sensing) or by statistically processing (e.g. by assuming spatial spectral distributions of the surface properties as done by *Dümenil and Todini* (1992) for the soil water capacities in their runoff/infiltration scheme).
- to define ‘effective’ parameters that represent the entire mosaic or the heterogeneity of a GCM grid cell (e.g. from aggregation of remotely sensed data at high resolution).
- to produce a simple flux aggregation (or upscaling) scheme that yields the spatially averaged flux densities over the entire mosaic or GCM grid cell.
- to produce a simple disaggregation (or downscaling) scheme that determines the land-atmosphere exchanges over each tile individually.

In this study we focus on the second approach. For the latter two approaches, see among others *Raupach* (1993).

In order to aggregate parameters to coarser resolutions most of the vegetation parameters (e. g. LAI, fractional coverages) can simply be linearly averaged, weighted by the fractional areas of the component land cover classes (*Feddes et al.*, 1998). For the roughness length  $z_{0,veg}$ , however, it has been found (e. g. *Mason*, 1988) that  $z_{0,veg}$  can best be logarithmically averaged at a so-called blending height (as described in Sect. 3.1).

#### 3.1. Aggregation of roughness length

As described in *Claussen et al.* (1994), the aggregation of roughness lengths from the 1 km scale to a coarser resolution by linear averaging is not valid. Therefore the concept of blending height is used. Instead of roughness values  $z_{0,veg}$ , drag coefficients  $c_d = (\kappa/\ln(z_b/z_{0,veg}))^2$  are averaged, where  $c_d$  are taken at the so-called blending height  $z_b$ . This leads to Eq. (4) for the aggregation within a gridbox:

$$\frac{1}{\ln^2\left(\frac{z_b}{z_{veg}}\right)} = \sum_j \left( \frac{f_j}{\ln^2\left(\frac{z_b}{z_{0,veg,j}}\right)} \right) \quad (4)$$

Here,  $f_j$  is the proportion of a gridbox covered with land cover type  $j$  and  $z_{0,veg,j}$  is the roughness length allocated to the land cover type  $j$ . We choose  $z_b = 100$  m as an order-of-magnitude guess according to *Claussen et al.* (1994).

## 4. Discussion of the new datasets

In Sect. 4.1, the new dataset of land surface parameters is compared to the old dataset. The comparison is done from a global point of view at the 0.5 degree resolution that is the highest resolution at which the old dataset is available. Sect. 4.2 deals with some aspects relevant for regional climate modelling over Europe and shows some features of the new dataset at a 0.1 degree resolution.

### 4.1. Global view

A major difference between the old and the new dataset is due to the fact that in the 1 km global ecosystem data the shelf ice region of Antarctica is classified as land (*glacier ice*), while in the old data this applies only to the continental land points. In the following figures, simple coastline data are used where the shelf ice is not included as land areas.

It is noticeable that the underlying resolution of the old parameter dataset is partly much coarser than 0.5 degree, which can be seen by means of large homogeneous blocks in e. g. South Africa and Australia, but also in many other parts of the earth as in South America and in Siberia.

Fig. 1a shows the new background albedo, and it is compared to the old background albedo (Fig. 1b) used in ECHAM4. Both datasets are able to depict many large scale features of the earth, such as the Congo basin, the Amazonian basin, the Tibetan high plateau, the Canadian and the North Asian boreal conifer forests. The new dataset apparently has an improved representation of the Scandinavian mountain ranges, the Andes and the Atacama desert in South America. Also the large desert regions in Australia seem to look more reasonable than in the old data. Only the new dataset resolves the Namib desert in South Africa, the Persian highlands, the Sierra Madre in Mexico, the Great Basin and the Great Plains in North America, the Gobi desert and the desert and mountain ranges north of Tibet. Most of these characteristics also apply to the other land surface parameters.

In the old albedo, the coastal regions of the Sahara and Saudi Arabia differ much from the central parts of the deserts. This difference does not exist in the new albedo data, but the new dataset seems to be realistic according to a desertification map of *Diercke* (1988, 1992).

The old global distribution of  $z_{0,veg}$  (Fig. 2b) has very rough transitions between regions with rather different values of  $z_{0,veg}$ . These transitions become smoother in the new data (Fig. 2a) so that more structures become visible. This is particularly the case for North America, the Amazonian basin and Central Africa.

For the new  $c_v$  (Fig. 3a), the most significant change from the old data (Fig. 3b) is caused by the large reduction of  $c_v$  for most ecosystem types related to conifer forests (especially the types 4, 21, 22, and 62, see Table 1 and 2). Therefore the boreal conifer forests of Canada and

northern Eurasia become less vegetated in the new mean  $c_v$ . The same applies to the new distributions of  $LAI$  (Fig. 4a) and  $c_f$  (Fig. 5) compared to the old distributions (Fig. 4b and 6), respectively. Additionally, the new distribution of  $c_f$  is more structured and the transitions between regions with rather different values of  $c_f$  are smoothed and thus improved as above.

To validate the quality of the parameter distributions of  $c_v$ ,  $LAI$  and  $c_f$ , global distributions of  $f_{PAR}$  are derived from  $c_v$  and  $LAI$  of the old and the new dataset using Eq. (1). These distributions are compared to the dataset of *Knorr* (1997, 1998) which will be referred to as surrogate data in the following. Due to a large amount of missing data (see also Sect. 2.3) in the surrogate dataset for the dormancy season, a graphical comparison to the new  $f_{PAR}$  data is only useful for the growing season. For this season, there is a large agreement between the new  $f_{PAR}$  (Fig. 7a) with the surrogate maximum  $f_{PAR}$  distribution (Fig. 7b). From this comparison it is evident that the reduction in  $c_v$  (as in  $LAI$  and  $c_f$ ) for northern conifer forests is realistic, since the new data have only slightly higher values of  $f_{PAR}$  in these regions than the surrogate data. The comparison between the mean distribution of  $f_{PAR}$  of the new (Fig. 8a) and the old data (Fig. 8b) reveals that the old data have much higher values in these regions which is not supported by the surrogate data.

The new distribution of  $W_{cap}$  (Fig. 9a) possesses considerably deeper soil reservoirs than the old water capacities (Fig. 9b) of *Patterson* (1990) used in ECHAM4, especially for latitudes below  $50^\circ$  N. Similar or slightly higher values are found north of  $50^\circ$  N, in Persia, in the Himalaya, in the North American east coast, in the Amazonian basin and the Congo basin. Lower values are found in the Sahara and in parts of Saudi Arabia, Canada and West Siberia.

The new distribution of  $W_{ava}$  (Fig. 10a) is similar to the surrogate data (Fig. 10b) of Kleidon (personal communication, 1998) in many regions of the earth. The surrogate data are biased with some noise which originates from the method to adapt the optimized rooting depth distribution to the climatic environment (cf. Sect. 2.5). Here, a spatially uncorrelated stochastic generation of daily precipitation (*Geng et al.*, 1986) derived from mean climate was used to construct the data. The noise is dominant in desert regions where only seldom but heavy precipitation events may occur. Despite of the noisy desert regions the new  $W_{ava}$  is very similar to the surrogate data in many regions of the world. Also in the noisy regions the new  $W_{ava}$  seems to be a smoothed version of the surrogate data. Larger differences exist in the eastern part of South America and in South Africa.

One general weakness of the 1 km satellite data is the particularly inadequate allocation of wetlands. Neither the Pantanal swamps and the wetlands in the Parana catchment in South America are well represented nor the wetlands surrounding the southern Hudson Bay, the wetlands in the Congo basin and in the East African highland lake area. This may be caused by the fact that the ecosystem types are allocated according to the major features of vegetation and land use. Thus, regions where the wetlands are only a secondary feature are not well characterized. While the other land surface parameters largely depend on the primary features of the land cover, the water capacity of the soil is strongly influenced if wetlands are present.

In many land surface parameterizations of atmospheric GCMs (among others *Chen et al.*, 1997), as, e.g., in ECHAM4, the soil water capacity defines the maximum amount of water that may be accumulated in the ground. Depending on the soil water capacity and the actual soil water content, the water that reaches the ground due to precipitation or snowmelt will partly infiltrate and runoff. A wetland (and also a lake) is actually an infinite reservoir that can store all the water which reaches the ground without a separation of runoff and infiltration, so that

the definition of a finite water capacity is not realistic. Because of this, the water capacity values assigned to wetlands ecosystem types (such as *Wooded Wet Swamp*, *Marsh Wetland* or *Mire, Bog, Fen*) are preliminary. The water capacity concept used in GCMs (see above) does not describe the physics of wetlands, although the values assigned to wetlands seem to be alright. In principle, a new approach is needed which describes the hydrologic behaviour over wetlands (and lakes). In this approach, wetlands should be treated separately in climate models (see also *Hagemann*, 1998) and will be taken care of in future model development.

For the mangrove swamp in the Niger delta, *Balogun and Oyebande* (1993) have measured that  $W_{cap}$  of the upper 100 cm of organic soil ranges from 48.6 to 53.2 cm. Since the values of  $W_{cap}$  considered in our study are not only related to the upper layer of soil, these values should be higher. This is the case for the new  $W_{cap}$  data in the Niger delta, but not for the old data where  $W_{cap}$  is less than 40 cm. This points to the fact that the assigned values of  $W_{cap}$  to the wetlands types may not be too unrealistic.

An accurate separation of lakes from the land ecosystem types is possible since a global distribution of fraction of land (or water) may be directly derived from the 1 km global dataset of ecosystem types (not shown). But the situation is different for wetlands. The currently best available global dataset for hydrological modelling that describes the fractional coverage by wetlands is a dataset of *Matthews and Fung* (1987) as indicated by results of *Hagemann and Dümenil* (1999). This dataset has a resolution of 1 degree which is certainly too coarse for regional climate modelling. An opportunity for the future may be the merging of this dataset with a wetlands distribution derived from the 1 km global ecosystem data.

## 4.2. Regional view at Europe

The most important feature of the new land surface parameter datasets is the very high resolution that may be obtained. Thus the datasets are particularly suitable for high resolution climate simulations as e. g. planned to be done for Europe in the MERCURE project. At MPI and DMI, the HIRHAM limited area model will be applied at resolutions of 0.44 and 0.22 degrees in a rotated lat-long grid. The 0.5 degree resolution of the old land surface datasets used in the MPI models (cf. Sect. 2) is clearly an insufficient resolution for a 0.22 degree model. But even for a 0.44 degree model for which this data resolution might be sufficient there are significant differences between the old and the new fields. As an example, Fig. 11 and Fig. 12 show the new and the old mean annual fractional vegetation in a non-rotated 0.5 degree grid. The new fields seem to be more realistic than the old ones. The Scandinavian mountain ranges have an improved structure and the Alps become visible in the new data. Also, the distribution of  $c_v$  is smoother without such harsh changes that occur in the old data, e. g. in Finland and eastern Europe. As shown in Sect. 4.1, similar and even larger improvements are found over other continents. This indicates that even for coarse resolution regional and global models the new fields of surface parameters may lead to significant improvements.

Fig. 13 and Fig. 14 show the new fields of seasonal fractional vegetation for summer and winter, respectively, at 0.1 degree resolution. Both figures illustrate that a high resolution is

needed in order to describe adequately the steep gradients, in particular those connected with the European mountain ranges. The figures also illustrate large seasonal variations in this parameter, ranging in many places up to 50-70%. Similar large variations are found in the leaf area index. In previous simulations with both the ECHAM model and the HIRHAM model mean annual values of both of these parameters have been used all year round. One of the new features that will be tried out in the planned experiments with the HIRHAM model will be to validate the effect of the introduction of seasonal varying surface fields. With the new high resolution parameter fields this seems feasible even for the highest resolution planned to be used in MERCURE.

For this seasonal variation, we suggest that  $c_v$  and  $LAI$  should range between the minimum and maximum values according to a function of subsoil temperature  $T_{soil}$  as shown in Eq. (5).

$$LAI = LAI_{min} + f(T_{soil}) \cdot (LAI_{max} - LAI_{min}) \quad (5)$$

The function  $f(T_{soil})$  is given in Eq. (6) where  $T_{soil}$  may range between a minimum temperature  $T_{min}$  and a maximum temperature  $T_{max}$ .

$$f(T_{soil}) = 1 - \left( \frac{T_{max} - T_{soil}}{T_{max} - T_{min}} \right)^2 \quad (6)$$

This approach is used in the BATS scheme (*Dickinson et al.*, 1993) and in the SECHIBA scheme (*Ducoudre et al.*, 1993). In BATS,  $T_{soil}$  is the temperature of the second layer of a 3 layer soil model with  $T_{min} = 273.1$  K and  $T_{max} = 298$  K. In SECHIBA,  $T_{soil}$  is the temperature of the fourth layer of a 7 layer soil model with  $T_{min} = 273$  K and  $T_{max} = 293$  K. For ECHAM4, we choose  $T_{soil}$  to be the third soil temperature layer (of 5), since the temperature used in Eq. (6) has to be independent of diurnal variations (*Schulz*, personal communication, 1998) that occur e. g. in the uppermost soil layer.

This approach considers only regions where the phenology of leaves and the growths of the vegetation is limited by temperature. In regions, where this is limited by water scarcity, such as in Spain or India, Eq. (6) is obviously not sufficient. The inclusion of the effects of water availability on  $c_v$  and  $LAI$  may be an important task for future improvements of the representation of the land surface in climate simulations.

## 5. Conclusions

An approach to construct new global datasets of land surface characteristics at resolutions down to 1 km was presented. They are derived from a 1 km global ecosystem distribution based on AVHRR satellite data. Compared to the currently available land surface data, the new datasets have a considerably improved resolution. Also at the same resolution as the old data, the new data show much more structures of the land surface and thus increase the quality of the land surface representation by gridded datasets.

Due to the finest resolution of 1 km that may be obtained, the new data seem to be very suitable for the application in very high resolution regional climate modelling as it is planned with the HIRHAM model. Also the inclusion of a seasonal cycle of  $c_v$  and  $LAI$  into climate models is possible, as it is suggested for ECHAM and HIRHAM.

The new parameter dataset is subject to improvements in some cases, especially regarding coarse resolution GCM applications. The soil water capacity distribution may be improved by using soil type information such as the 0.5 degree soil type dataset of *Dunne and Wilmott* (1996) based on *FAO/Unesco* (1971-1981). Although very high resolution soil type data are currently not globally available, the existing data may be used to correct the  $W_{cap}$  data for coarse resolution GCM applications. Soil surface albedo information would be useful to improve the background albedo distribution in bare soil regions, such as in the Sahara and Saudi Arabia.

## Acknowledgements

We thank Jens Hesselberg Christensen and Ole Bossing Christensen from the Danish Meteorological Institute for fruitful discussions about the 1 km ecosystem data and their technical processing. We are grateful to Axel Kleidon from the MPI who has prepared the surrogate dataset of  $W_{ava}$  we have used to allocate ecosystem types with water capacity values. He has also provided some insight into the issue of deep roots and soil reservoirs. We wish to thank Wolfgang Knorr from the MPI who has provided the global dataset of  $f_{PAR}$  and who has supported us with valuable information about  $LAI$  and  $c_v$ . This study was supported by funding from the European Union within the MERCURE (Modelling European Regional Climate: Understanding and Reducing Errors) project (contract No. ENV4-CT97-0485).

## References

- Balogun, I., and L. Oyebande, 1993  
Physical and hydrological processes of Niger delta wetland soils  
In: Bolle, H.-J., R.A. Feddes and J.D. Kalma (Eds.): Exchange Processes at the Land Surface for a Range of Space and Time Scales  
(Proceedings of the Yokohama Symposium, July 1993), *IAHS Publ.* **212**, 273-280
- Barkstrom, B.R., E.F. Harrison and R.B. Lee, 1990  
Earth Radiation Budget Experiment, Preliminary seasonal results  
*EOS Transactions*, American Geophysical Union, **71**, February 27
- Batjes, N.H., 1996  
Development of a world data set of soil water retention properties using pedotransfer rules  
*Geoderma*, **71**, 31-52
- Bergström, S., 1992  
The HBV model - its structure and applications  
*Swedish Meteorological and Hydrological Institute Rep.* **4**
- Berthelot, B., G. Dedieu, F. Cabot and S. Adam, 1994  
Estimation of surface reflectance and vegetation index using NOAA/AVHRR: Methods and results at global scale  
*Communication for the 6th international symposium on physical measurements and signatures in remote sensing*, ISPRS, Wal d'Isere, France, 17-21 January
- Canadell, J., R.B. Jackson, J.R. Ehleringer, H.A. Mooney, O.E. Sala and E.-D. Schulze, 1996  
Maximum rooting depth of vegetation types at the global scale  
*Oecologia*, **108** (4), 583-595
- Chen, T. H., A. Henderson-Sellers, P. C. D. Milly, A. J. Pitman, A. C. M. Beljaars, J. Polcher, F. Abramopoulos, A. Boone, S. Chang, F. Chen, Y. Dai, C. E. Desborough, R. E. Dickinson, L. Dümenil, M. Ek, J. R. Garratt, N. Gedney, Y. M. Gusev, J. Kim, R. Koster, E. A. Kowalczyk, K. Laval, J. Lean, D. Lettenmaier, X. Liang, J.-F. Mahfouf, H.-T. Mengelkamp, K. Mitchell, O. N. Nasonova, J. Noilhan, A. Robock, C. Rosenzweig, J. Schaake, C. A. Schlosser, J.-P. Schulz, Y. Shao, A. B. Shmakin, D. L. Verseghy, P. Wetzell, E. F. Wood, Y. Xue, Z.-L. Yang und Q. Zeng, 1997:  
Cabauw experimental results from the project for intercomparison of land-surface parameterization schemes  
*J. Climate* **10**, 1194-1215.
- Christensen, J.H., Christensen, O.B., Lopez, P., van Meijgaard, E., and Botzet, M., 1996  
The HIRHAM 4 regional atmospheric climate model  
DMI Scientific Report **96-4**, Copenhagen, Denmark
- Claussen, M., 1991  
Estimation of areally-averaged surface fluxes  
*Boundary-Layer Meteorology* **54**, 387-410
- Claussen, M., U. Lohmann, E. Roeckner and U. Schulzweida, 1994  
A global dataset of land surface parameters  
*Max-Planck-Institute for Meteorology, Report* **135**, Hamburg, Germany
- Cogley, J.G., 1986  
THYDRO: A terrestrial hydrographic data set

(submitted)

- Cogley, J.G., (1987, 1991, 1994)  
*GGHYDRO - Global Hydrographic Data, Release 2.1*,  
Department of Geography, Trent University, Peterborough, Ontario, Canada
- Dickinson, R.E., A. Henderson-Sellers and P.J. Kennedy, 1993  
Biosphere-Atmosphere Transfer Scheme (BATS) version 1e as coupled to the NCAR  
community climate model  
NCAR Technical Note **387**, Boulder, Colorado
- Diercke, 1988, 1992  
Weltatlas  
Westermann Schulbuchverlag GmbH, Braunschweig
- Ducoudre, N.I., K. Laval and A. Perrier, 1993  
SECHIBA, a new set of parameterizations of the hydrologic exchanges at the land-  
atmosphere interface within the LMD atmospheric general circulation model  
*J. Climate* **6**, 248-273
- Dümenil, L., und E. Todini, 1992  
A rainfall-runoff scheme for use in the Hamburg climate model  
In: J.P. Kane (Ed.): *Advances in Theoretical Hydrology - a Tribute to James Dooge*,  
Elsevier Science Publishers, 129-157
- Dunne, K.A., and C.J. Willmott, 1996  
Global distribution of plant-extractable water capacity of soil  
*Int. J. Climatol.* **16**, 841-859
- Eidenshink, J. C., and J. L. Faundeen, 1994  
The 1 km AVHRR global land data set: First stages in implementation  
*Int. J. Remote Sens.* **15**, (no. 17): 3443-3462
- FAO/Unesco, 1971-1981  
Soil map of the world  
Vols. 1-10, Unesco, Paris
- Feddes, R.A., P. Kabat, A.J. Dolman, R.W.A. Hutjes and M.J. Waterloo, 1998  
Large-scale field experiments to improve land surface parameterisations  
In: R. Lemmelä and N. Helenius (Eds.): *Proceedings of 'The Second International  
Conference on Climate and Water'*, Espoo, Finland, 17-20 August 1998: 619-646
- Geng, S., F. Penning de Vries and I. Supit, 1986  
A simple method for generating daily rainfall data  
*Agric. For. Meteorol.* **36**, 363-376
- Gildea, M.P., and B. Moore, 1986  
FAOSOL - A global soils archive  
Durham, New Hampshire: Complex Systems Research Center, University of New  
Hampshire (unpublished data tape and documentation)
- Hagemann, S., and L. Dümenil, 1999  
Comparison of two global wetlands datasets using a global hydrological discharge model.  
Submitted to *Hydrology and Earth System Sciences*
- Hagemann, S., and A. Kleidon, 1998  
The influence of rooting depth on the simulated hydrological cycle of a GCM

- submitted to *Physics and Chemistry of the Earth*
- Henderson-Sellers, A., M.F. Wilson, G. Thomas and R.E. Dickinson, 1986  
Current global land-surface data sets for use in climate-related studies  
NCAR Technical Note **272**, Boulder, Colorado
- Jacob, D., and R. Podzun, 1997  
Sensitivity studies with the regional climate model REMO  
*Meteorology and Atmospheric Physics* **63**: 119-129
- Kleidon, A., and M. Heimann, 1998a  
Optimised rooting depth and its impacts on the simulated climate of an atmospheric general circulation model  
*Geophys. Res. Lett.*, **25**(3): 345-348.
- Kleidon, A., and M. Heimann, 1998b  
The effect of deep rooted vegetation on the simulated climate of an atmospheric general circulation model. Part I: Mechanism and comparison to observations  
submitted to *Clim. Dyn.*
- Kleidon, A., and M. Heimann, 1998c  
A method of determining rooting depth from a terrestrial biosphere model and its impacts on the global water- and carbon cycle  
*Global Change Biology*, **4** (3), 275-286
- Knorr, W., 1997  
Satellitengestützte Fernerkundung und Modellierung des globalen CO<sub>2</sub>-Austauschs der Landvegetation: Eine Synthese  
Examensarbeit 49, Max-Planck-Institute for Meteorology, Hamburg, Germany
- Knorr, W., 1998  
Constraining a global mechanistic vegetation model with satellite data.  
In: 'IEEE International Geoscience and Remote Sensing Symposium' Proceedings, Seattle, WA, 6-10 July 1998.
- Mason, P.J., 1987  
On the parameterization of orographic drag  
In: Seminar / workshop 1986 - Observation, theory and modelling of orographic effects, Vol. **1**, ECMWF, Reading, UK, 167-194
- Mason, P.J., 1988  
The formation of areally-averaged roughness lengths  
*Q. J. R. Meteorol. Soc.* **114**: 399-420
- Matthews, E., 1983  
Global vegetation and land use: New high resolution data bases for climate studies  
*J. Clim. Appl. Meteor.* **22**, 474-487
- Matthews, E., and I. Fung, 1987  
Methane emissions from natural wetlands: Global distribution, area, and environmental characteristics of sources  
*Global Biogeochem. Cycles* **1**, 61-86
- Meeson, B.W., F.E. Corprew, J.M.P. McManus, D.M. Myers, J.W. Closs, K.-J. Sun, D.J. Sunday and P.J. Sellers, 1995  
ISLSCP initiative I - global data sets for land-atmosphere models, 1987-1988  
Volumes 1-5. Published on CD by NASA

- Monsi, M., and T. Saeki, 1953  
 Über den Lichtfaktor in den Pflanzengesellschaften und seine Bedeutung für die Stoffproduktion  
*Japanese Journal of Botany* **14**: 22-52
- Olson, J.S., 1994a  
 Global ecosystem framework-definitions  
 USGS EROS Data Center Internal Report, Sioux Falls, SD
- Olson, J.S., 1994b  
 Global ecosystem framework-translation strategy  
 USGS EROS Data Center Internal Report, Sioux Falls, SD
- Olson, J.S., J.A. Watts and L.J. Allison, 1983  
 Carbon in live vegetation of major world ecosystems  
 ORNL-5862, Oak Ridge National Laboratory, Oak Ridge
- Patterson, K.A., 1990  
 Global distributions of total and total-avaiable soil water-holding capacities  
 Master's thesis, University of Delaware, Newark, DE
- Pielke, R.A., T.J. Lee, J.H. Copeland, J.L. Eastman, C.L. Ziegler and C.A. Finley, 1997  
 Use of USGS-provided data to improve weather and climate simulations  
*Ecological Applications* **7** (1): 3-21
- Ramanathan, V., R.D. Cess, E.F. Harrison, P. Minis, B.R. Barkstrom, E. Ahmad and D. Hartmann, 1989  
 Cloud-radiative forcing and climate: results from the Earth Radiation Budget Experiment  
*Science* **243**: 57-63
- Raupach, M.R., 1993  
 The averaging of surface flux densities  
 In: Bolle, H.-J., R.A. Feddes and J.D. Kalma (Eds.): Exchange Processes at the Land surface for a range of space and time scales (Proceedings of the Yokohama Symposium, July 1993), IAHS Publ. **212**: 343-355
- Roeckner, E., K. Arpe, L. Bengtsson, M. Christoph, M. Claussen, L. Dümenil, M. Esch, M. Giorgetta, U. Schlese and U. Schulzweida, 1996  
 The atmospheric general circulation model ECHAM-4: model description and simulation of present-day climate  
*Max-Planck-Institute for Meteorology, Report* **218**, Hamburg, Germany
- Rowntree, P.R., 1991  
 Atmospheric parameterization schemes for evaporation over land: basic concepts and climate modelling aspects  
 In: Schmugge, T.J. and J. Andre (Eds.): *Land Surface Evaporation - Measurement and Parameterization*, Springer Verlag, S. 5-29
- Schulz, J.-P., L. Dümenil, J. Polcher, C. A. Schlosser and Y. Xue, 1998  
 Land surface energy and moisture fluxes: comparing three models  
*J. Appl. Meteor.* **37**, 288-307
- Sellers, P.J., D.A. Randall, C.J. Collatz, J.A. Berry, C.B. Field, D.A. Dazlich, C. Zhang, and C.D. Collelo, 1995a  
 A revised land surface parameterization (SiB2) for atmospheric GCMs. Part 1: Model formulation

submitted to *J. Climate*

Sellers, P.J., S.O. Los, C.J. Tucker, C.O. Justice, D.A. Dazlich, G.J. Collatz, and D.A. Randall, 1995b.

A revised land surface parameterization (SiB2) for atmospheric GCMs. Part 2: The generation of global fields of terrestrial biophysical parameters from satellite data.

Submitted to *J. Climate*

Tibaldi, S., and J.-F. Geleyn, 1981

The production of a new orography, land-sea mask and associated climatological surface fields for operational purposes

ECMWF Technical Memorandum **40**

U.S. Geological Survey, 1997

Global land cover characteristics data base

[http://edcwww.cr.usgs.gov/landdaac/glcc/globe\\_int.html](http://edcwww.cr.usgs.gov/landdaac/glcc/globe_int.html)

Warrilow, D.A., A.B. Sangster and A. Slingo, 1986

Modelling of land surface processes and their influence on European climate

Dynamical Climatology Technical Note **38**

Wilson, M.F., 1984

Construction and use of land surface information in a general circulation climate model

Unpublished Ph.D. Thesis, University of Liverpool

Wilson, M.F., and A. Henderson-Sellers, 1985

A global archive of land cover and soil data for use in general circulation models

*J. Climatol.*, **5**, 119-143

## Tables and Figures

**Table 1:** Initial parameter values based solely on *Claussen et al. (1994)*

Global ecosystem types of *Olson (1994a, 1994b)* that correspond almost directly to one of the old types of *Olson et al. (1983)* are marked with a \*. In the USGS dataset, there is no separation between *Inland Water (14)* and *Sea Water (15)* since all water gridboxes are marked as type 14. Several of the new ecosystem types introduced in *Olson (1994a, 1994b)* do not occur in the satellite dataset, so that they are excluded from the table: *Mixed Forest and Field (18)*, *Cold Irrigated Cropland (39)*, *Volcanic Rock (49)*, *Coastal Wetland in NW (65)*, *NE (66)*, *SE (67)* and *SW (68)*, *Glacier Rock (70)*, *Salt Playas (71)*, *Water and Island Fringe (73)*, *Land, Water, and Shore (74)*, *Land and Water, Rivers (75)*, *Southern Hemisphere Conifers (77)*, *Wet Sclerophylic Forest (79)*, *Coastline Fringe (80)*, *Beaches and Dunes (81)*, *Sparse Dunes and Ridges (82)*, *Bare Coastal Dunes (83)*, *Residual Dunes and Beaches (84)*, *Compound Coastlines (85)*, *Rocky Cliffs and Slopes (86)*, *Sandy Grassland and Shrubs (87)*, *Bamboo (88)*. The roughness length  $z_{0,veg}$  is given in m.

| Type | Global Ecosystems Legend      | $a_s$ | $z_{0,veg}$ | $c_v g$ | $c_v d$ | LAI g | LAI d | $c_f$ |
|------|-------------------------------|-------|-------------|---------|---------|-------|-------|-------|
| 1    | Urban                         | 0.2   | 2.5         | 0.      | 0.      | 0.    | 0.    | 0.    |
| 2    | Low Sparse Grassland          | 0.19  | 0.03        | 0.44    | 0.      | 1.5   | 0.1   | 0.    |
| 3    | Coniferous Forest             | 0.13  | 1.          | 0.96    | 0.95    | 9.2   | 9.0   | 0.9   |
| 4    | Deciduous Conifer Forest      | 0.13  | 1.          | 0.76    | 0.      | 3.8   | 0.1   | 0.9   |
| 5    | Deciduous Broadleaf Forest    | 0.16  | 1.          | 0.88    | 0.      | 5.2   | 0.1   | 0.85  |
| 6 *  | Evergreen Broadleaf Forests   | 0.16  | 0.68        | 0.99    | 0.97    | 9.9   | 9.5   | 0.95  |
| 7    | Tall Grasses and Shrubs       | 0.2   | 0.1         | 0.44    | 0.      | 1.5   | 0.1   | 0.    |
| 8    | Bare Desert                   | 0.28  | 0.005       | 0.      | 0.      | 0.    | 0.    | 0.    |
| 9 *  | Upland Tundra                 | 0.17  | 0.03        | 0.55    | 0.      | 2.1   | 0.    | 0.    |
| 10   | Irrigated Grassland           | 0.16  | 0.03        | 0.9     | 0.1     | 4.5   | 0.    | 0.    |
| 11   | Semi Desert                   | 0.28  | 0.005       | 0.15    | 0.      | 0.5   | 0.    | 0.    |
| 12 * | Glacier Ice                   | 0.7   | 0.005       | 0.      | 0.      | 0.    | 0.    | 0.    |
| 13   | Wooded Wet Swamp              | 0.12  | 0.03        | 0.73    | 0.67    | 3.5   | 3.0   | 0.    |
| 14 * | Water                         | 0.07  | 0.0002      | 0.      | 0.      | 0.    | 0.    | 0.    |
| 16   | Shrub Evergreen               | 0.165 | 0.55        | 0.9     | 0.3     | 6.    | 3.    | 0.5   |
| 17   | Shrub Deciduous               | 0.16  | 0.26        | 0.85    | 0.      | 4.7   | 0.1   | 0.4   |
| 19   | Evergreen Forest and Fields   | 0.16  | 0.25        | 0.9     | 0.3     | 6.    | 3.    | 0.5   |
| 20   | Cool Rain Forest              | 0.12  | 2.          | 0.96    | 0.96    | 9.3   | 9.3   | 0.95  |
| 21   | Conifer Boreal Forest         | 0.13  | 1.          | 0.91    | 0.91    | 6.    | 6.    | 0.8   |
| 22 * | Cool Conifer Forest           | 0.13  | 1.          | 0.96    | 0.95    | 9.2   | 9.0   | 0.9   |
| 23 * | Cool Mixed Forest             | 0.15  | 1.          | 0.76    | 0.      | 3.8   | 0.1   | 0.8   |
| 24   | Mixed Forest                  | 0.16  | 0.68        | 0.93    | 0.3     | 7.    | 1.    | 0.8   |
| 25   | Cool Broadleaf Forest         | 0.16  | 1.          | 0.88    | 0.      | 5.2   | 0.1   | 0.85  |
| 26   | Deciduous Broadleaf Forest    | 0.16  | 1.          | 0.88    | 0.      | 5.2   | 0.1   | 0.85  |
| 27   | Conifer Forest                | 0.13  | 1.          | 0.99    | 0.97    | 9.9   | 9.5   | 0.95  |
| 28 * | Montane Tropical Forests      | 0.15  | 0.55        | 0.86    | 0.77    | 4.8   | 4.0   | 0.5   |
| 29 * | Seasonal Tropical Forest      | 0.12  | 2.          | 0.91    | 0.6     | 6.    | 2.5   | 0.9   |
| 30 * | Cool Crops and Towns          | 0.18  | 0.1         | 0.9     | 0.      | 2.5   | 0.    | 0.    |
| 31   | Crops and Town                | 0.18  | 0.1         | 0.9     | 0.1     | 4.5   | 1.    | 0.    |
| 32 * | Dry Tropical Woods            | 0.14  | 0.55        | 0.91    | 0.6     | 6.0   | 2.5   | 0.6   |
| 33 * | Tropical Rainforest           | 0.12  | 2.          | 0.96    | 0.96    | 9.3   | 9.3   | 0.95  |
| 34   | Tropical Degraded Forest      | 0.14  | 0.55        | 0.91    | 0.6     | 6.0   | 2.5   | 0.6   |
| 35   | Corn and Beans Cropland       | 0.18  | 0.1         | 0.9     | 0.      | 2.5   | 0.    | 0.    |
| 36 * | Rice Paddy and Field          | 0.15  | 0.06        | 0.9     | 0.1     | 4.5   | 0.    | 0.    |
| 37 * | Hot Irrigated Cropland        | 0.18  | 0.05        | 0.6     | 0.      | 4.    | 0.    | 0.    |
| 38 * | Cool Irrigated Cropland       | 0.18  | 0.05        | 0.6     | 0.      | 3.    | 0.    | 0.    |
| 40 * | Cool Grasses and Shrubs       | 0.19  | 0.06        | 0.44    | 0.      | 1.5   | 0.    | 0.    |
| 41 * | Hot and Mild Grasses & Shrubs | 0.2   | 0.1         | 0.44    | 0.      | 1.5   | 0.1   | 0.    |
| 42   | Cold Grassland                | 0.19  | 0.03        | 0.44    | 0.      | 1.5   | 0.    | 0.    |
| 43 * | Savanna (Woods)               | 0.16  | 0.25        | 0.53    | 0.3     | 1.9   | 1.0   | 0.4   |
| 44 * | Mire, Bog, Fen                | 0.12  | 0.03        | 0.6     | 0.      | 2.5   | 0.1   | 0.    |
| 45   | Marsh Wetland                 | 0.12  | 0.03        | 0.6     | 0.      | 2.5   | 0.1   | 0.    |
| 46 * | Mediterranean Scrub           | 0.15  | 0.46        | 0.8     | 0.67    | 4.3   | 3.0   | 0.4   |

| Type | Global Ecosystems Legend       | $a_s$ | $z_{0,veg}$ | $c_v$ g | $c_v$ d | LAI g | LAI d | $c_f$ |
|------|--------------------------------|-------|-------------|---------|---------|-------|-------|-------|
| 47 * | Dry Woody Scrub                | 0.16  | 0.26        | 0.85    | 0.      | 4.7   | 0.1   | 0.4   |
| 48   | Dry Evergreen Woods            | 0.18  | 0.04        | 0.34    | 0.      | 1.2   | 0.    | 0.3   |
| 50 * | Sand Desert                    | 0.28  | 0.005       | 0.      | 0.      | 0.    | 0.    | 0.    |
| 51 * | Semi Desert Shrubs             | 0.28  | 0.005       | 0.15    | 0.      | 0.5   | 0.    | 0.    |
| 52   | Semi Desert Sage               | 0.28  | 0.005       | 0.15    | 0.      | 0.5   | 0.    | 0.    |
| 53 * | Barren Tundra                  | 0.17  | 0.03        | 0.55    | 0.      | 2.1   | 0.    | 0.    |
| 54   | Cool South. Hemi. Mix-Forests  | 0.16  | 0.65        | 0.86    | 0.      | 4.8   | 0.1   | 0.8   |
| 55 * | Cool Fields and Woods          | 0.19  | 0.1         | 0.9     | 0.1     | 3.    | 0.    | 0.3   |
| 56 * | Forest and Field               | 0.18  | 0.17        | 0.9     | 0.3     | 6.    | 3.    | 0.5   |
| 57 * | Cool Forest and Field          | 0.18  | 0.17        | 0.9     | 0.2     | 4.    | 1.    | 0.5   |
| 58 * | Fields and Woody Savanna       | 0.19  | 0.1         | 0.9     | 0.2     | 5.    | 2.    | 0.3   |
| 59 * | Succulent and Thorn Scrub      | 0.2   | 0.03        | 0.86    | 0.3     | 4.8   | 1.    | 0.4   |
| 60   | Small Leaf Mixed Woods         | 0.15  | 1.          | 0.76    | 0.      | 3.8   | 0.1   | 0.8   |
| 61   | Deciduous & Mix. Boreal Forest | 0.16  | 0.65        | 0.86    | 0.      | 4.8   | 0.1   | 0.8   |
| 62   | Narrow Conifers                | 0.15  | 0.31        | 0.73    | 0.      | 3.5   | 0.1   | 0.4   |
| 63 * | Wooded Tundra                  | 0.18  | 0.05        | 0.7     | 0.15    | 3.2   | 0.5   | 0.2   |
| 64 * | Heath Scrub                    | 0.2   | 0.1         | 0.85    | 0.      | 4.7   | 0.1   | 0.    |
| 69 * | Polar and Alpine Desert        | 0.28  | 0.005       | 0.      | 0.      | 0.    | 0.    | 0.    |
| 72 * | Mangrove                       | 0.12  | 1.29        | 0.95    | 0.95    | 9.    | 9.    | 0.9   |
| 76   | Crop and Water Mixtures        | 0.15  | 0.06        | 0.9     | 0.1     | 4.5   | 0.    | 0.    |
| 78   | Southern Hemi. Mixed Forest    | 0.16  | 0.65        | 0.86    | 0.      | 4.8   | 0.1   | 0.8   |
| 89   | Moist Eucalyptus               | 0.16  | 0.65        | 0.86    | 0.      | 4.8   | 0.1   | 0.8   |
| 90 * | Rain Green Tropical Forest     | 0.12  | 2.          | 0.96    | 0.96    | 9.3   | 9.3   | 0.95  |
| 91 * | Woody Savanna                  | 0.16  | 0.25        | 0.53    | 0.3     | 1.9   | 1.0   | 0.4   |
| 92   | Broadleaf Crops                | 0.17  | 0.175       | 0.9     | 0.2     | 5.    | 2.    | 0.3   |
| 93   | Grass Crops                    | 0.185 | 0.065       | 0.72    | 0.      | 2.    | 0.    | 0.    |
| 94   | Crops, Grass, Shrubs           | 0.19  | 0.1         | 0.9     | 0.1     | 3.    | 0.    | 0.    |

**Table 2:** Corrected and improved parameter values

As in Table 1, ecosystem types not occurring in the satellite dataset are excluded from the table.  $W_{ava}$  is given in mm and  $z_{0,veg}$  in m.

| Type | Global Ecosystems Legend      | $a_s$ | $z_{0,veg}$ | $c_v g$ | $c_v d$ | $LAI g$ | $LAI d$ | $c_f$ | $W_{ava}$ | $f_{pwp}$ |
|------|-------------------------------|-------|-------------|---------|---------|---------|---------|-------|-----------|-----------|
| 1    | Urban                         | 0.2   | 2.5         | 0.      | 0.      | 0.      | 0.      | 0.    | 0.        | 0.48      |
| 2    | Low Sparse Grassland          | 0.19  | 0.03        | 0.53    | 0.04    | 1.75    | 0.12    | 0.    | 580.      | 0.45      |
| 3    | Coniferous Forest             | 0.13  | 1.          | 0.96    | 0.95    | 9.2     | 9.0     | 0.9   | 130.      | 0.41      |
| 4    | Deciduous Conifer Forest      | 0.13  | 1.          | 0.56    | 0.      | 3.6     | 0.1     | 0.56  | 155.      | 0.45      |
| 5    | Deciduous Broadleaf Forest    | 0.16  | 1.          | 0.88    | 0.      | 5.2     | 0.1     | 0.85  | 240.      | 0.53      |
| 6    | Evergreen Broadleaf Forests   | 0.16  | 0.68        | 0.99    | 0.97    | 9.9     | 9.5     | 0.95  | 220.      | 0.38      |
| 7    | Tall Grasses and Shrubs       | 0.2   | 0.1         | 0.7     | 0.26    | 2.2     | 0.76    | 0.    | 590.      | 0.35      |
| 8    | Bare Desert                   | 0.28  | 0.005       | 0.      | 0.      | 0.      | 0.      | 0.    | 100.      | 0.        |
| 9    | Upland Tundra                 | 0.17  | 0.03        | 0.64    | 0.07    | 2.3     | 0.4     | 0.    | 60.       | 0.33      |
| 10   | Irrigated Grassland           | 0.16  | 0.03        | 0.9     | 0.1     | 4.5     | 0.      | 0.    | 450.      | 0.49      |
| 11   | Semi Desert                   | 0.28  | 0.005       | 0.1     | 0.      | 0.46    | 0.      | 0.    | 45.       | 0.51      |
| 12   | Glacier Ice                   | 0.7   | 0.005       | 0.      | 0.      | 0.      | 0.      | 0.    | 0.        | 0.        |
| 13   | Wooded Wet Swamp              | 0.12  | 0.03        | 0.73    | 0.67    | 3.5     | 3.0     | 0.    | 235.      | 0.50      |
| 14   | Water                         | 0.07  | 0.0002      | 0.      | 0.      | 0.      | 0.      | 0.    | 0.        | 0.        |
| 16   | Shrub Evergreen               | 0.165 | 0.55        | 0.6     | 0.22    | 6.      | 2.2     | 0.35  | 800.      | 0.46      |
| 17   | Shrub Deciduous               | 0.16  | 0.26        | 0.45    | 0.08    | 4.6     | 0.45    | 0.22  | 140.      | 0.33      |
| 19   | Evergreen Forest and Fields   | 0.16  | 0.25        | 0.78    | 0.3     | 6.      | 3.      | 0.3   | 200.      | 0.47      |
| 20   | Cool Rain Forest              | 0.12  | 2.          | 0.96    | 0.96    | 9.3     | 9.3     | 0.95  | 70.       | 0.34      |
| 21   | Conifer Boreal Forest         | 0.13  | 1.          | 0.5     | 0.5     | 5.5     | 5.5     | 0.44  | 185.      | 0.32      |
| 22   | Cool Conifer Forest           | 0.13  | 1.          | 0.7     | 0.35    | 9.2     | 4.4     | 0.66  | 380.      | 0.49      |
| 23   | Cool Mixed Forest             | 0.15  | 1.          | 0.95    | 0.02    | 4.2     | 0.1     | 0.95  | 140.      | 0.40      |
| 24   | Mixed Forest                  | 0.16  | 0.68        | 0.93    | 0.3     | 7.      | 1.      | 0.8   | 300.      | 0.51      |
| 25   | Cool Broadleaf Forest         | 0.16  | 1.          | 0.88    | 0.17    | 5.2     | 0.51    | 0.85  | 210.      | 0.43      |
| 26   | Deciduous Broadleaf Forest    | 0.16  | 1.          | 0.88    | 0.26    | 5.2     | 0.79    | 0.85  | 250.      | 0.51      |
| 27   | Conifer Forest                | 0.13  | 1.          | 0.87    | 0.31    | 9.7     | 4.4     | 0.84  | 250.      | 0.49      |
| 28   | Montane Tropical Forests      | 0.15  | 0.55        | 0.86    | 0.77    | 4.8     | 4.0     | 0.5   | 630.      | 0.47      |
| 29   | Seasonal Tropical Forest      | 0.12  | 2.          | 0.99    | 0.71    | 9.1     | 2.74    | 0.98  | 200.      | 0.52      |
| 30   | Cool Crops and Towns          | 0.18  | 0.1         | 0.9     | 0.36    | 2.5     | 1.85    | 0.    | 310.      | 0.50      |
| 31   | Crops and Town                | 0.18  | 0.1         | 0.9     | 0.16    | 4.5     | 1.1     | 0.    | 450.      | 0.50      |
| 32   | Dry Tropical Woods            | 0.14  | 0.55        | 0.96    | 0.22    | 6.1     | 2.5     | 0.63  | 470.      | 0.46      |
| 33   | Tropical Rainforest           | 0.12  | 2.          | 0.96    | 0.96    | 9.3     | 9.3     | 0.95  | 235.      | 0.52      |
| 34   | Tropical Degraded Forest      | 0.14  | 0.55        | 0.86    | 0.24    | 5.96    | 2.4     | 0.57  | 460.      | 0.50      |
| 35   | Corn and Beans Cropland       | 0.18  | 0.1         | 0.9     | 0.08    | 2.5     | 0.4     | 0.    | 250.      | 0.495     |
| 36   | Rice Paddy and Field          | 0.15  | 0.06        | 0.95    | 0.1     | 4.6     | 0.      | 0.    | 350.      | 0.49      |
| 37   | Hot Irrigated Cropland        | 0.18  | 0.05        | 0.8     | 0.25    | 4.4     | 1.3     | 0.    | 390.      | 0.51      |
| 38   | Cool Irrigated Cropland       | 0.18  | 0.05        | 0.6     | 0.      | 3.      | 0.      | 0.    | 370.      | 0.48      |
| 40   | Cool Grasses and Shrubs       | 0.19  | 0.06        | 0.6     | 0.01    | 1.9     | 0.05    | 0.    | 480.      | 0.42      |
| 41   | Hot and Mild Grasses & Shrubs | 0.2   | 0.1         | 0.53    | 0.17    | 1.71    | 0.5     | 0.    | 680.      | 0.44      |
| 42   | Cold Grassland                | 0.19  | 0.03        | 0.94    | 0.18    | 1.5     | 2.89    | 0.    | 270.      | 0.52      |
| 43   | Savanna (Woods)               | 0.16  | 0.25        | 0.95    | 0.25    | 3.      | 0.91    | 0.4   | 900.      | 0.47      |
| 44   | Mire, Bog, Fen                | 0.12  | 0.03        | 0.6     | 0.      | 2.5     | 0.1     | 0.    | 120.      | 0.38      |
| 45   | Marsh Wetland                 | 0.12  | 0.03        | 0.6     | 0.      | 2.5     | 0.1     | 0.    | 800.      | 0.55      |
| 46   | Mediterranean Scrub           | 0.15  | 0.46        | 0.8     | 0.2     | 4.3     | 2.5     | 0.4   | 480.      | 0.54      |
| 47   | Dry Woody Scrub               | 0.16  | 0.26        | 0.8     | 0.26    | 4.6     | 0.8     | 0.38  | 600.      | 0.47      |
| 48   | Dry Evergreen Woods           | 0.18  | 0.04        | 0.6     | 0.3     | 1.8     | 1.7     | 0.53  | 400.      | 0.46      |
| 50   | Sand Desert                   | 0.28  | 0.005       | 0.      | 0.      | 0.      | 0.      | 0.    | 100.      | 0.        |
| 51   | Semi Desert Shrubs            | 0.28  | 0.005       | 0.27    | 0.1     | 0.83    | 0.56    | 0.    | 500.      | 0.40      |
| 52   | Semi Desert Sage              | 0.28  | 0.005       | 0.39    | 0.      | 1.18    | 0.      | 0.    | 860.      | 0.425     |
| 53   | Barren Tundra                 | 0.17  | 0.03        | 0.19    | 0.      | 1.89    | 0.      | 0.    | 60.       | 0.30      |
| 54   | Cool South. Hemi. Mix-Forests | 0.16  | 0.65        | 0.86    | 0.      | 4.8     | 0.1     | 0.8   | 80.       | 0.45      |
| 55   | Cool Fields and Woods         | 0.19  | 0.1         | 0.9     | 0.2     | 3.      | 0.9     | 0.3   | 140.      | 0.445     |
| 56   | Forest and Field              | 0.18  | 0.17        | 0.97    | 0.2     | 6.1     | 2.2     | 0.54  | 180.      | 0.47      |
| 57   | Cool Forest and Field         | 0.18  | 0.17        | 0.9     | 0.2     | 4.      | 1.      | 0.5   | 230.      | 0.485     |
| 58   | Fields and Woody Savanna      | 0.19  | 0.1         | 0.95    | 0.28    | 5.1     | 2.1     | 0.32  | 620.      | 0.51      |
| 59   | Succulent and Thorn Scrub     | 0.2   | 0.03        | 0.56    | 0.19    | 4.7     | 0.92    | 0.26  | 820.      | 0.43      |

| Type | Global Ecosystems Legend       | $a_s$ | $z_{0,veg}$ | $c_v g$ | $c_v d$ | $LAI g$ | $LAI d$ | $c_f$ | $W_{ava}$ | $f_{pwp}$ |
|------|--------------------------------|-------|-------------|---------|---------|---------|---------|-------|-----------|-----------|
| 60   | Small Leaf Mixed Woods         | 0.15  | 1.          | 0.53    | 0.      | 3.69    | 0.1     | 0.53  | 240.      | 0.39      |
| 61   | Deciduous & Mix. Boreal Forest | 0.16  | 0.65        | 0.57    | 0.      | 4.7     | 0.1     | 0.53  | 140.      | 0.495     |
| 62   | Narrow Conifers                | 0.15  | 0.31        | 0.53    | 0.      | 3.38    | 0.1     | 0.29  | 240.      | 0.34      |
| 63   | Wooded Tundra                  | 0.18  | 0.05        | 0.55    | 0.15    | 3.07    | 0.5     | 0.16  | 85.       | 0.35      |
| 64   | Heath Scrub                    | 0.2   | 0.1         | 0.5     | 0.      | 4.6     | 0.1     | 0.    | 90.       | 0.45      |
| 69   | Polar and Alpine Desert        | 0.28  | 0.005       | 0.      | 0.      | 0.      | 0.      | 0.    | 35.       | 0.43      |
| 72   | Mangrove                       | 0.12  | 1.29        | 0.95    | 0.95    | 9.      | 9.      | 0.9   | 290.      | 0.50      |
| 76   | Crop and Water Mixtures        | 0.15  | 0.06        | 0.65    | 0.12    | 4.4     | 0.16    | 0.    | 2000.     | 0.575     |
| 78   | Southern Hemi. Mixed Forest    | 0.16  | 0.65        | 0.8     | 0.      | 4.7     | 0.1     | 0.75  | 235.      | 0.40      |
| 89   | Moist Eucalyptus               | 0.16  | 0.65        | 0.85    | 0.55    | 4.8     | 2.8     | 0.8   | 270.      | 0.55      |
| 90   | Rain Green Tropical Forest     | 0.12  | 2.          | 0.96    | 0.96    | 9.3     | 9.3     | 0.95  | 360.      | 0.42      |
| 91   | Woody Savanna                  | 0.16  | 0.25        | 0.53    | 0.33    | 1.9     | 1.06    | 0.4   | 490.      | 0.50      |
| 92   | Broadleaf Crops                | 0.17  | 0.175       | 0.94    | 0.25    | 5.      | 2.3     | 0.31  | 360.      | 0.49      |
| 93   | Grass Crops                    | 0.185 | 0.065       | 0.72    | 0.      | 2.      | 0.      | 0.    | 140.      | 0.47      |
| 94   | Crops, Grass, Shrubs           | 0.19  | 0.1         | 0.67    | 0.2     | 2.7     | 0.8     | 0.    | 490.      | 0.465     |

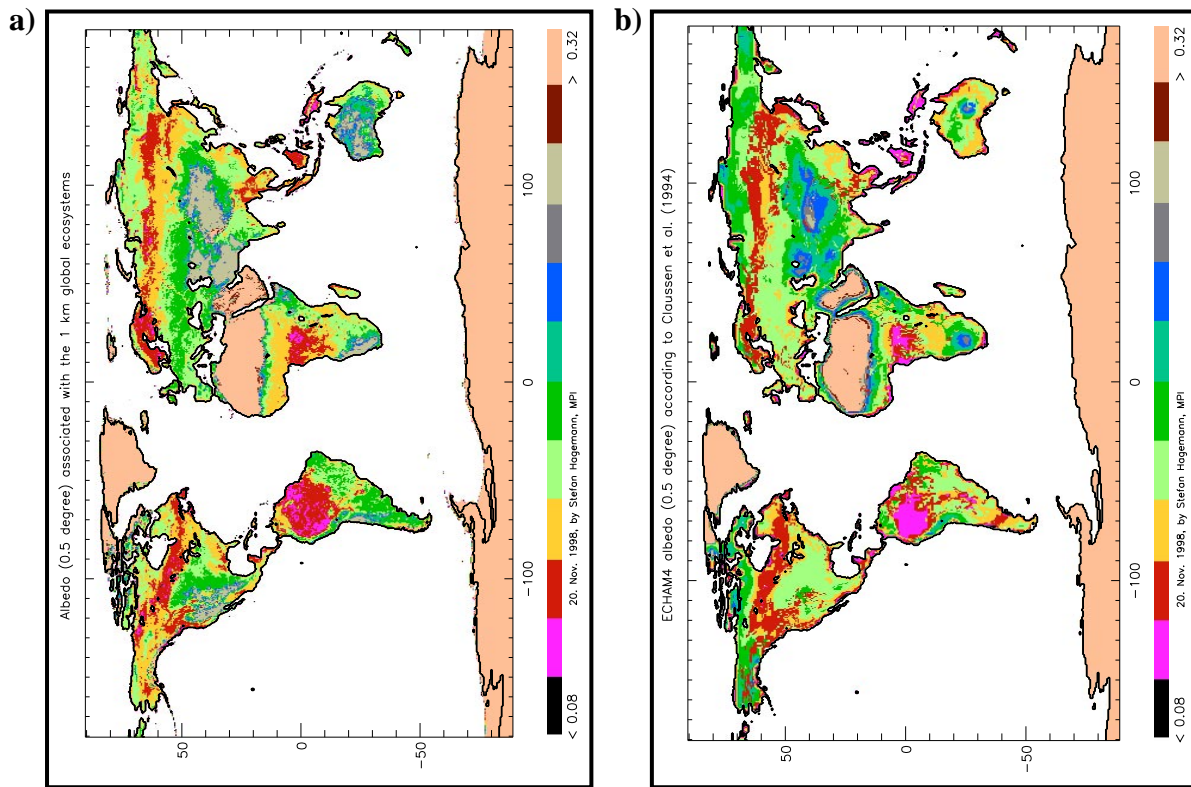


**Fig. 1.** Background albedo at 0.5 degree resolution that is a) associated with the 1 km ecosystem data (*Water* is assigned an albedo of 0.07), and b) used in ECHAM4 according to *Claussen et al.* (1994) (*Water* is assigned an albedo of 0). Colour scale in 0.02 steps.

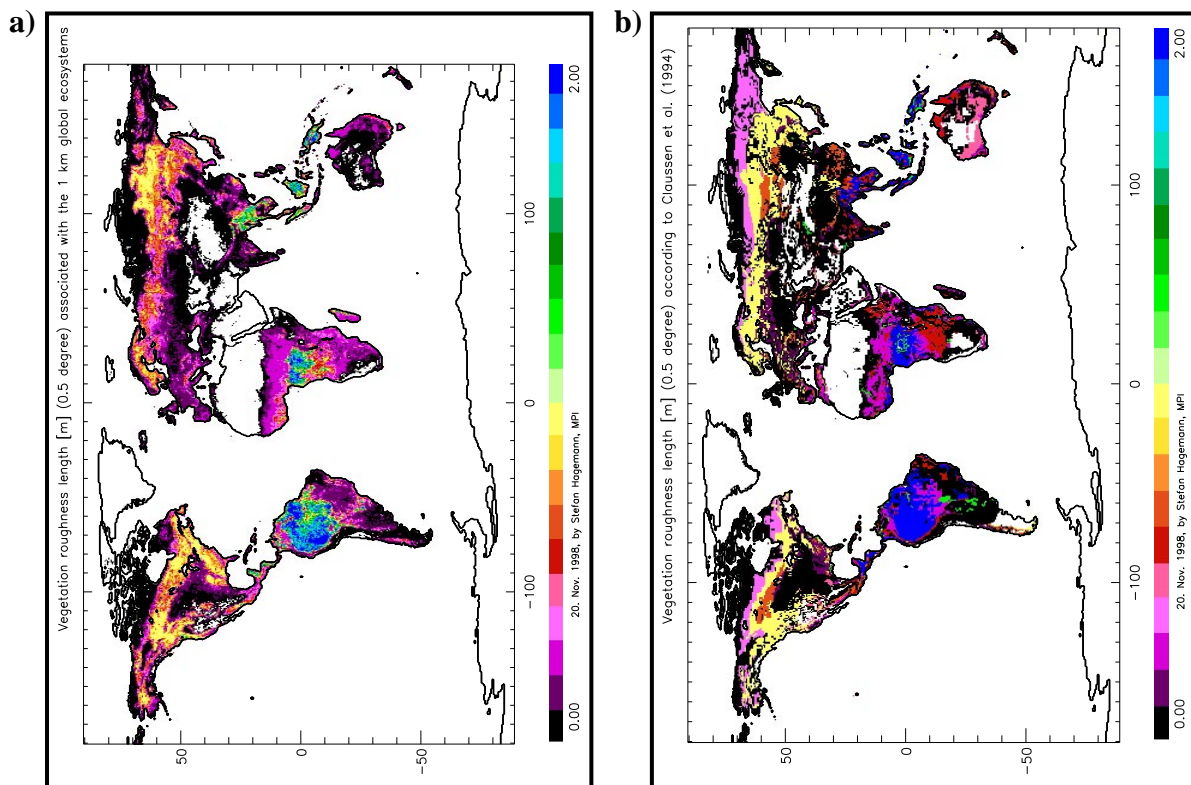


**Fig. 2.** Roughness length due to vegetation and land use at 0.5 degree resolution that is a) associated with the 1 km ecosystem data, and b) used in ECHAM4 according to *Claussen et al.* (1994). Colour scale in 0.1 m steps.

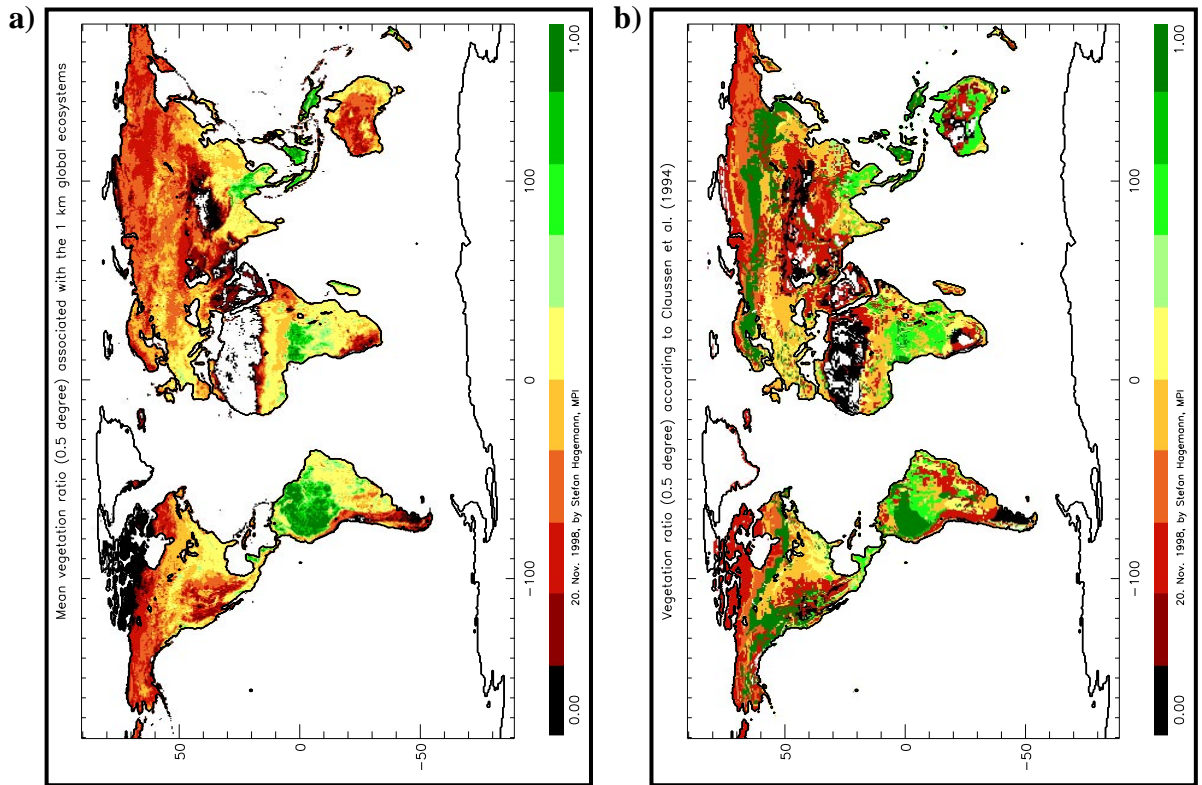


**Fig. 3.** Fractional vegetation at 0.5 degree resolution that is **a)** associated with the 1 km ecosystem data, and **b)** used in ECHAM4 according to *Claussen et al.* (1994). Colour scale in 10% steps.

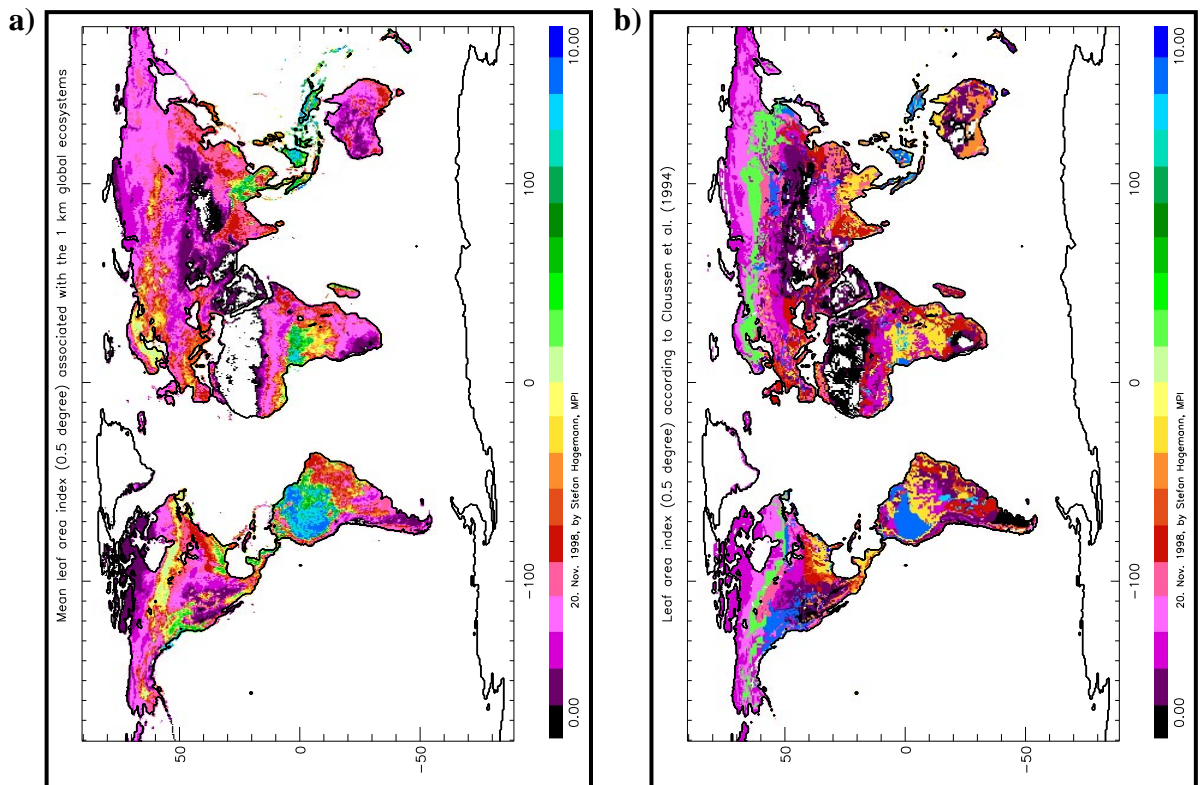


**Fig. 4.** Mean leaf area index at 0.5 degree resolution that is **a)** associated with the 1 km ecosystem data, and **b)** used in ECHAM4 according to *Claussen et al.* (1994). Colour scale in 0.5 steps.

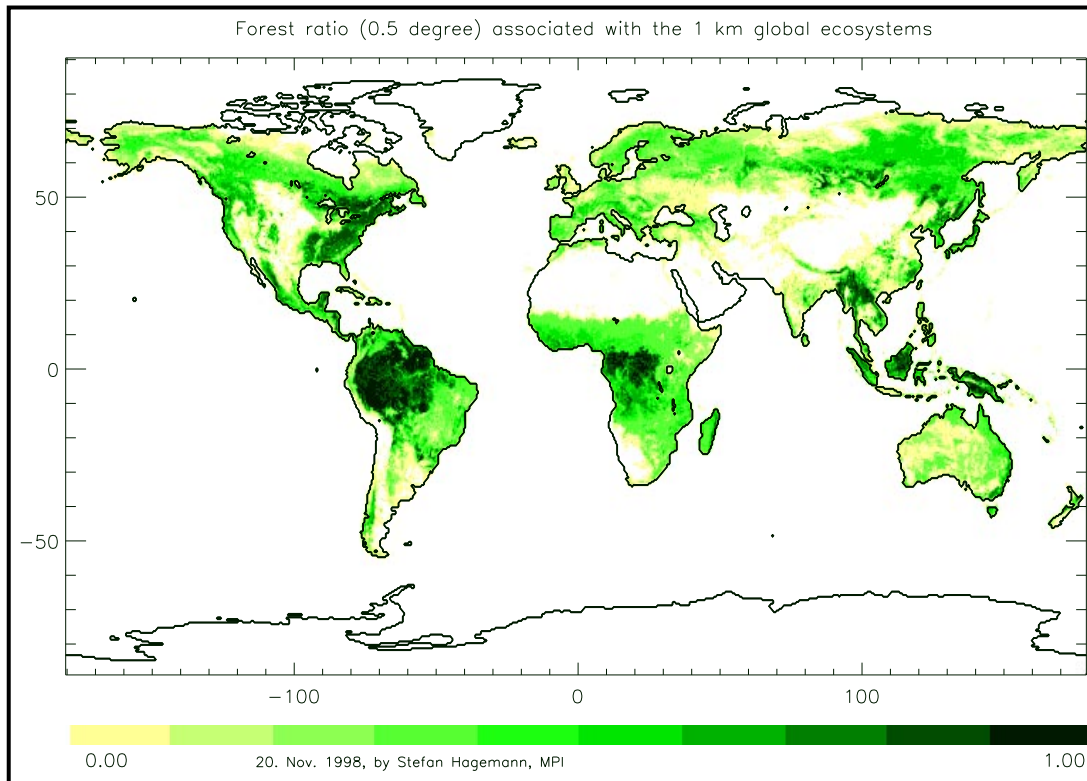


**Fig. 5.** Forest ratio at 0.5 degree resolution associated with the 1 km ecosystem data. Gray scale in 10% steps.

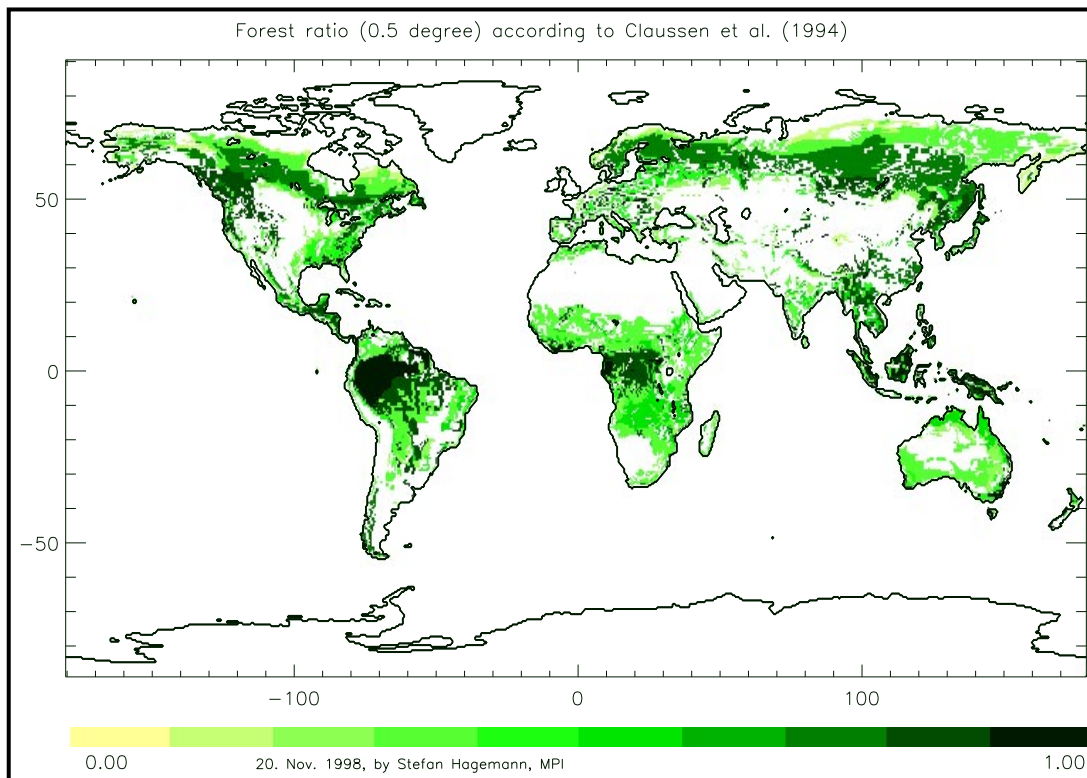


**Fig. 6.** Forest ratio at 0.5 degree resolution that is used in ECHAM4 according to *Claussen et al.* (1994). Gray scale in 10% steps.

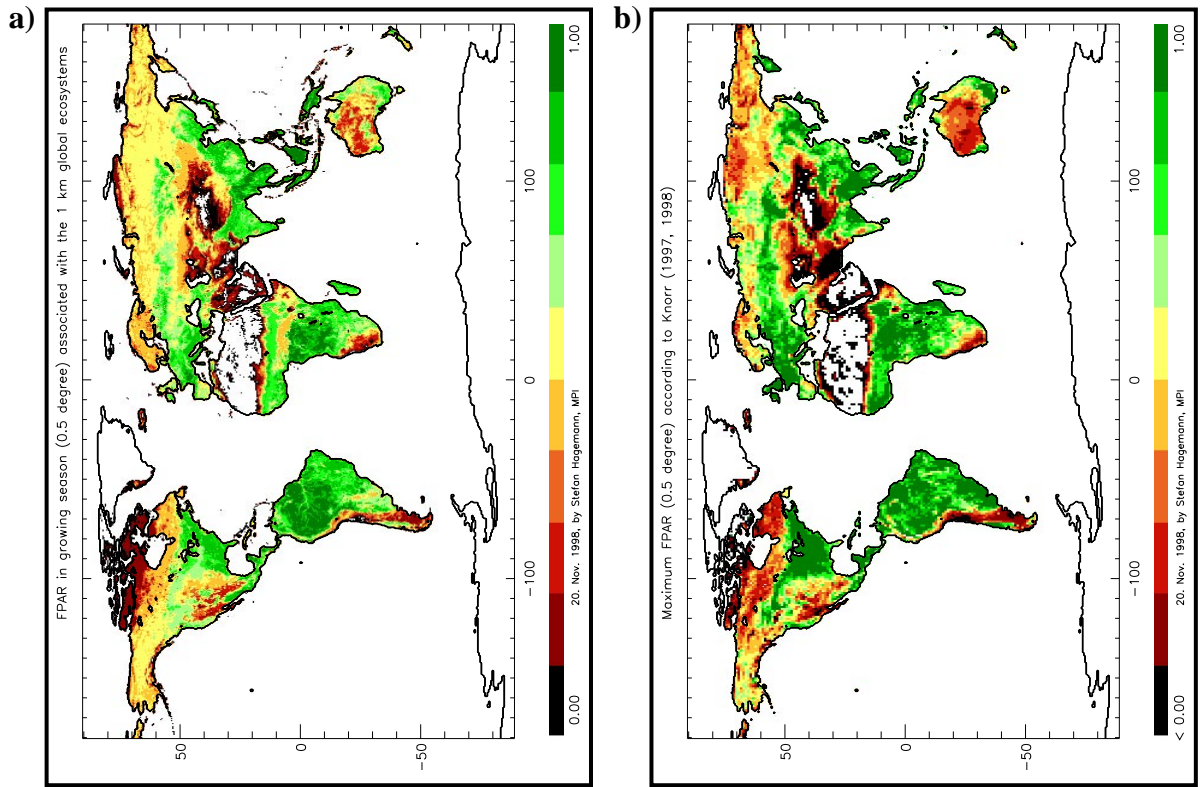


**Fig. 7.**  $f_{PAR}$  in the growing season at 0.5 degree resolution that is **a)** associated with the 1 km ecosystem data, and **b)** maximum  $f_{PAR}$  according to *Knorr* (1997, 1998). Colour scale in 10% steps.

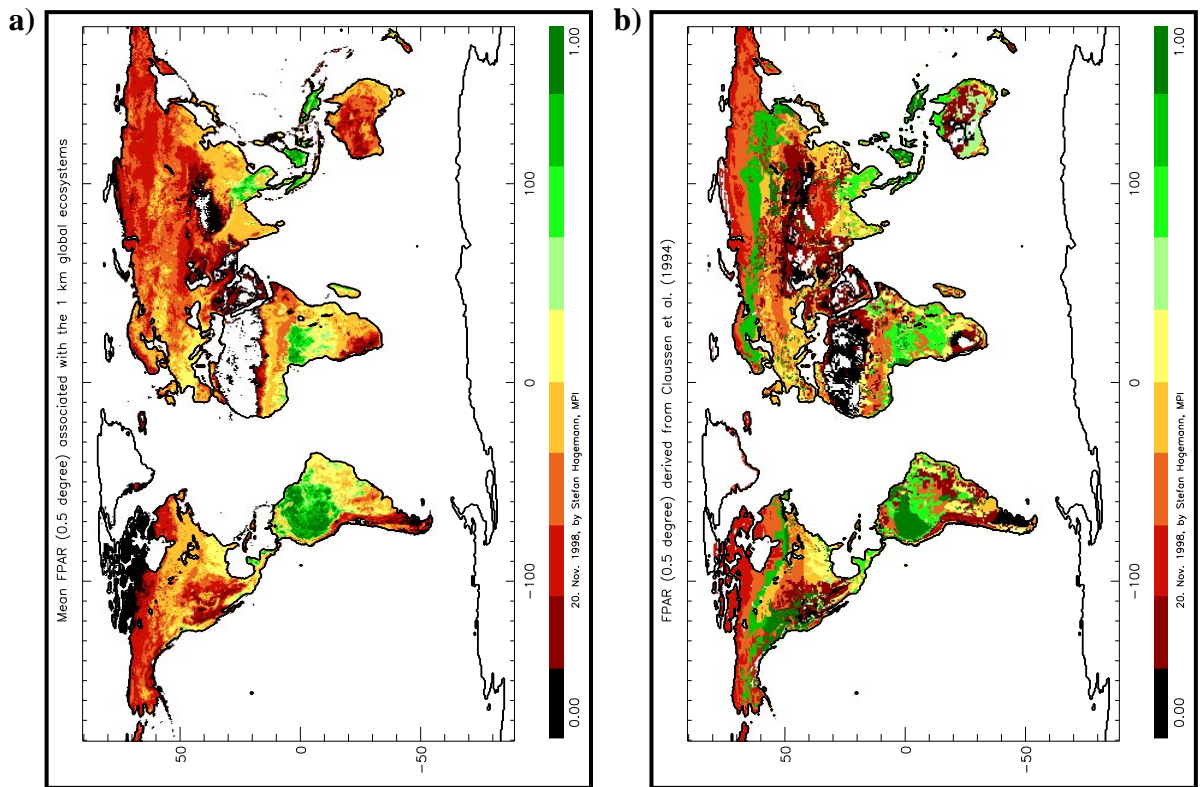


**Fig. 8.** Mean  $f_{PAR}$  at 0.5 degree resolution associated with the **a)** 1 km ecosystem data, and **b)** *Claussen et al.* (1994). Colour scale in 10% steps.

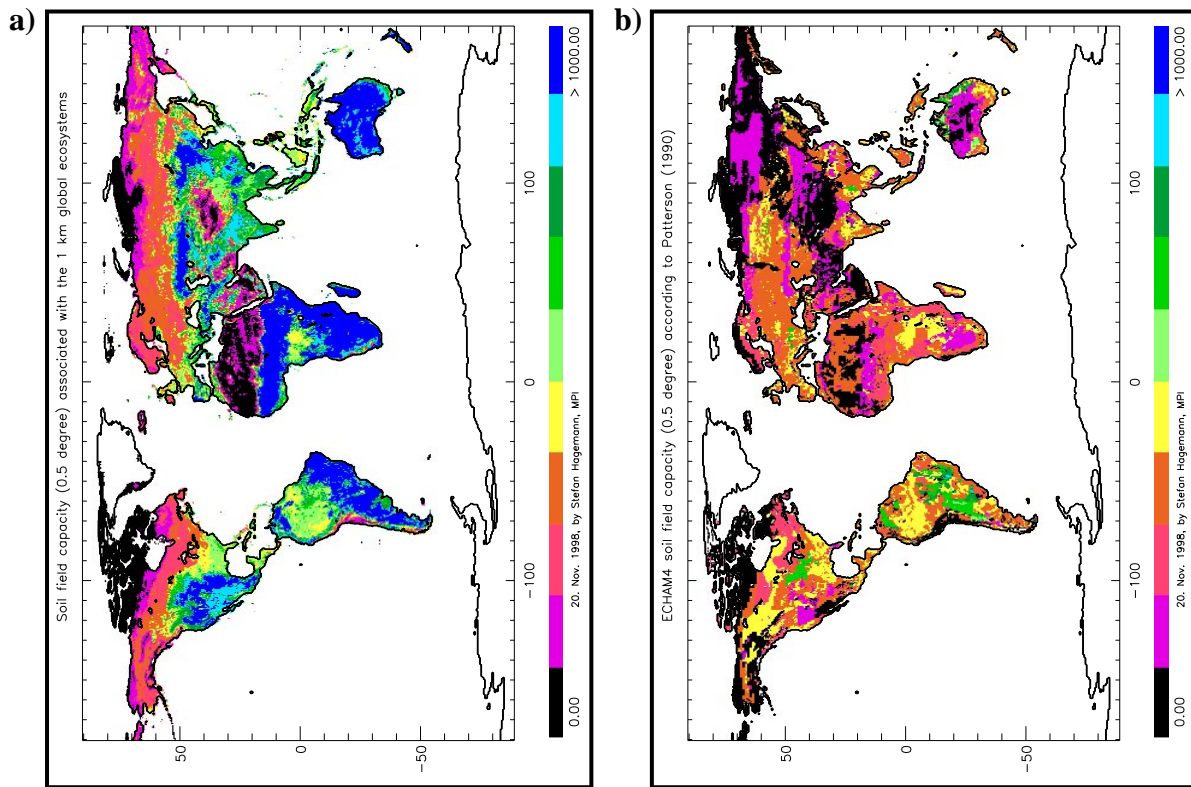


**Fig. 9.** Soil field capacity at 0.5 degree resolution that is **a)** associated with the 1 km ecosystem data, and **b)** used in ECHAM4 according to *Patterson* (1990). Colour scale in 100 mm steps.

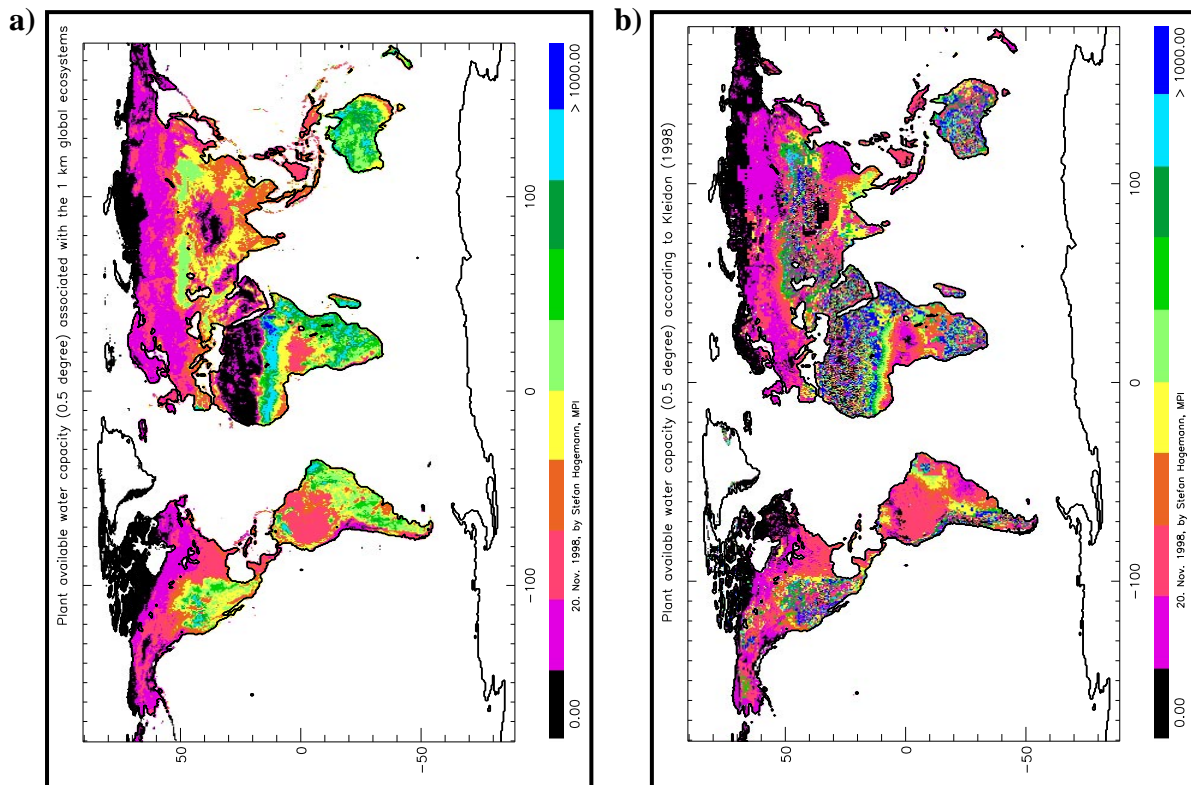


**Fig. 10.** Plant available water capacity at 0.5 degree resolution **a)** associated with the 1 km ecosystem data, and **b)** according to *Kleidon* (1998). Colour scale in 100 mm steps.

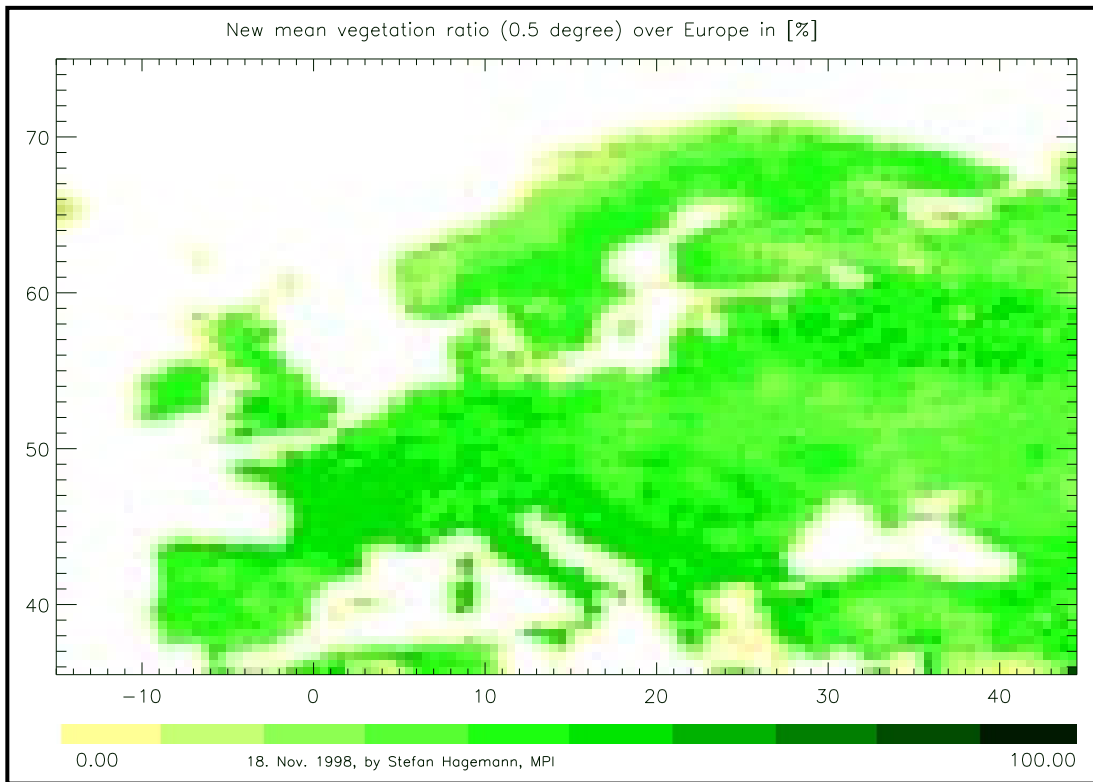


**Fig. 11.** New mean fractional vegetation associated with the 1 km ecosystem data at 0.5 degree resolution. Gray scale in 10% steps.

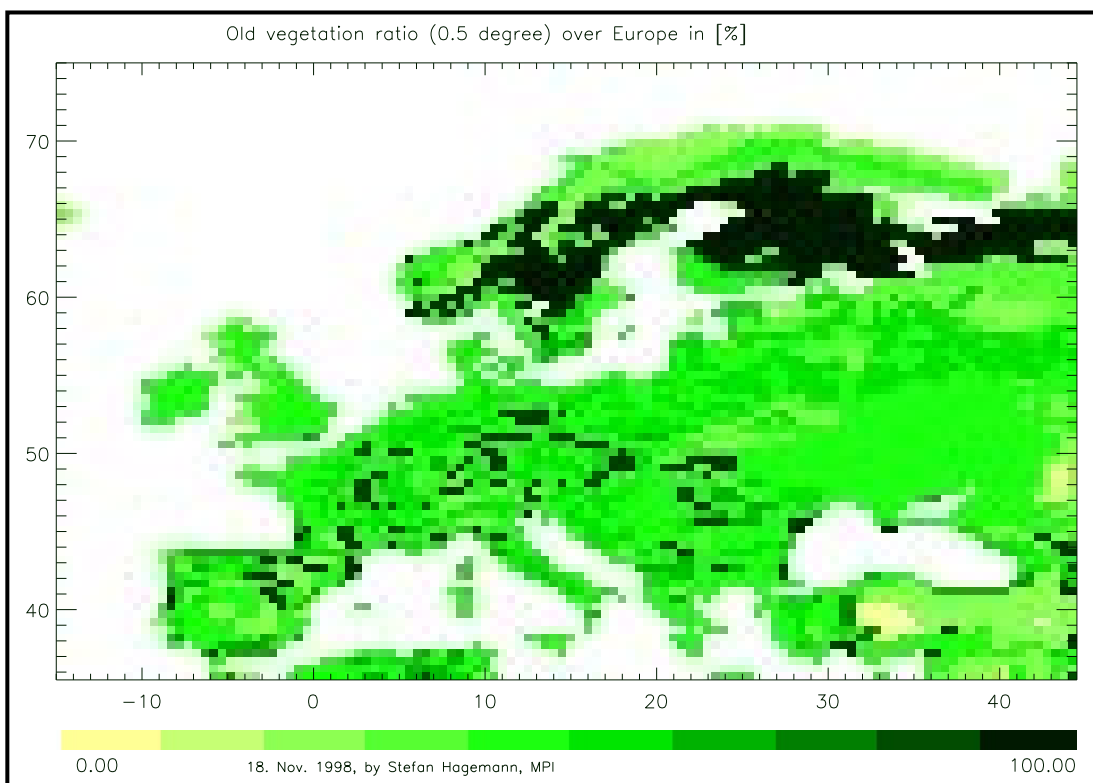


**Fig. 12.** Old fractional vegetation according to *Claussen et al.* (1994) at 0.5 degree resolution. Gray scale in 10% steps.

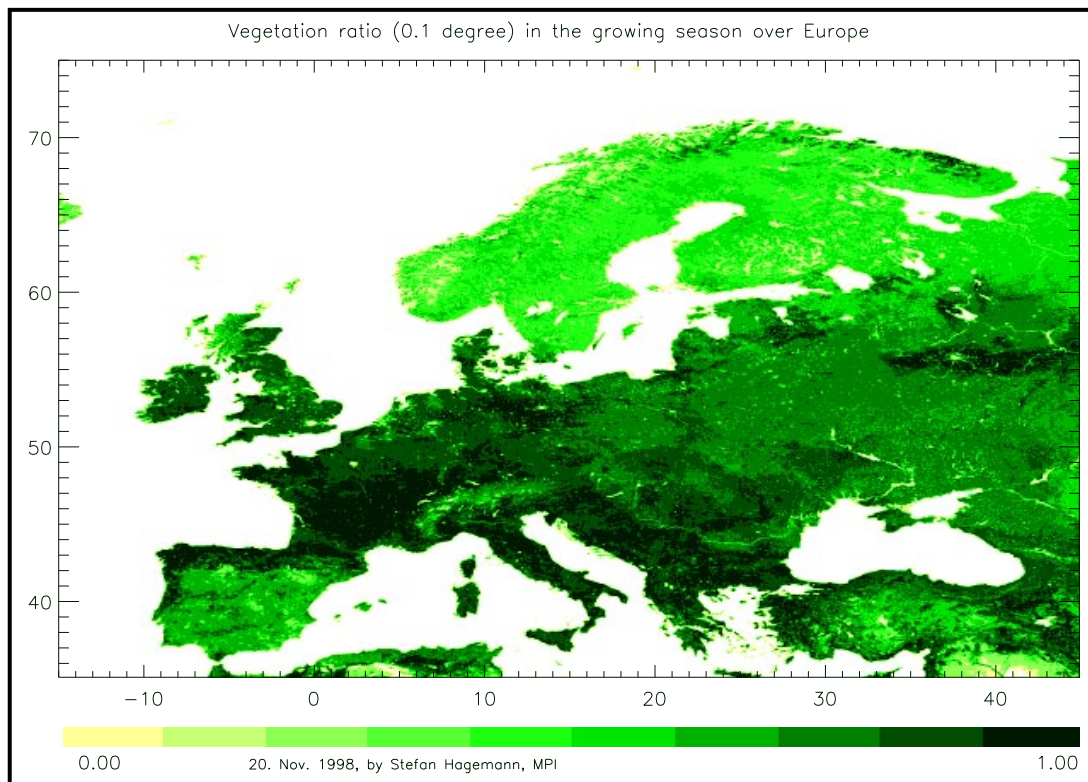


**Fig. 13.** Vegetation ratio in the growing season associated with the 1 km ecosystem data at 0.1 degree resolution. Gray scale in 10% steps.

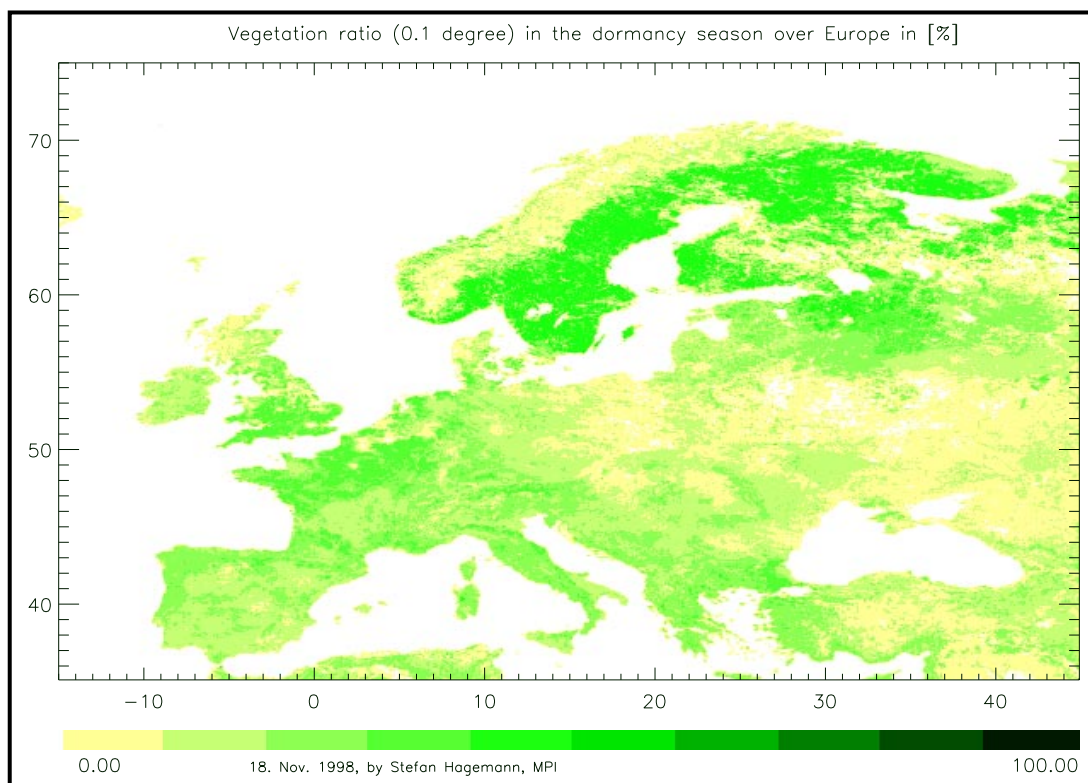


**Fig. 14.** Vegetation ratio in the dormancy season associated with the 1 km ecosystem data at 0.1 degree resolution. Gray scale in 10% steps.